Electronic Supplementary Material (ESI) for Journal of Materials Chemistry C.

Supporting Information

Novel Titania Organic/ Inorganic Hybrids via Simultaneous ROMP and Sol-gel Chemistries

Johannes A. van Hensbergen; Robert P. Burford* & Andrew B. Lowe*

Centre for Advanced Macromolecular Design (CAMD). School of Chemical Engineering, University of New South Wales, Sydney N.S.W. 2052. Australia.

Table of Contents

1. Additional SEM images
    - 1.1 Unetched polymers and hybrids
    - 1.2 HF etched polymers and hybrids
    - 1.3 Pyrolysis chars
2. Additional TEM images
3. Additional TGA traces
4. Additional DMA traces
5. FTIR spectra of polymers and hybrids
6. Raman spectra of TES hybrids and titania controls

1. Additional SEM images

1.1 Unetched polymers and hybrids

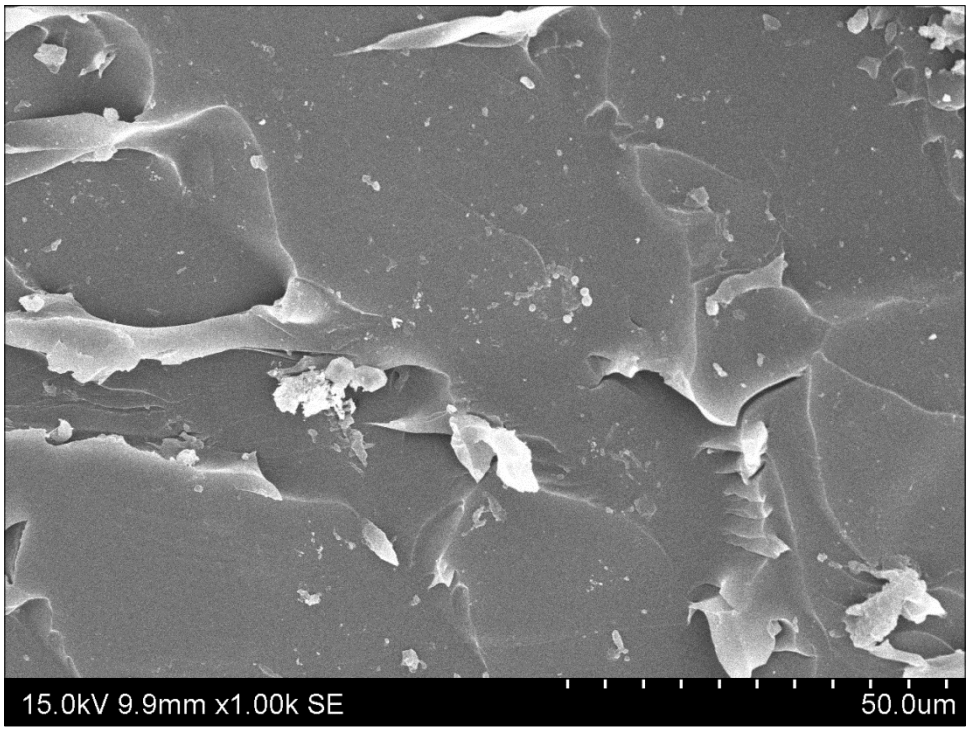

Figure S1: Polynorbornene (**PNBE**)

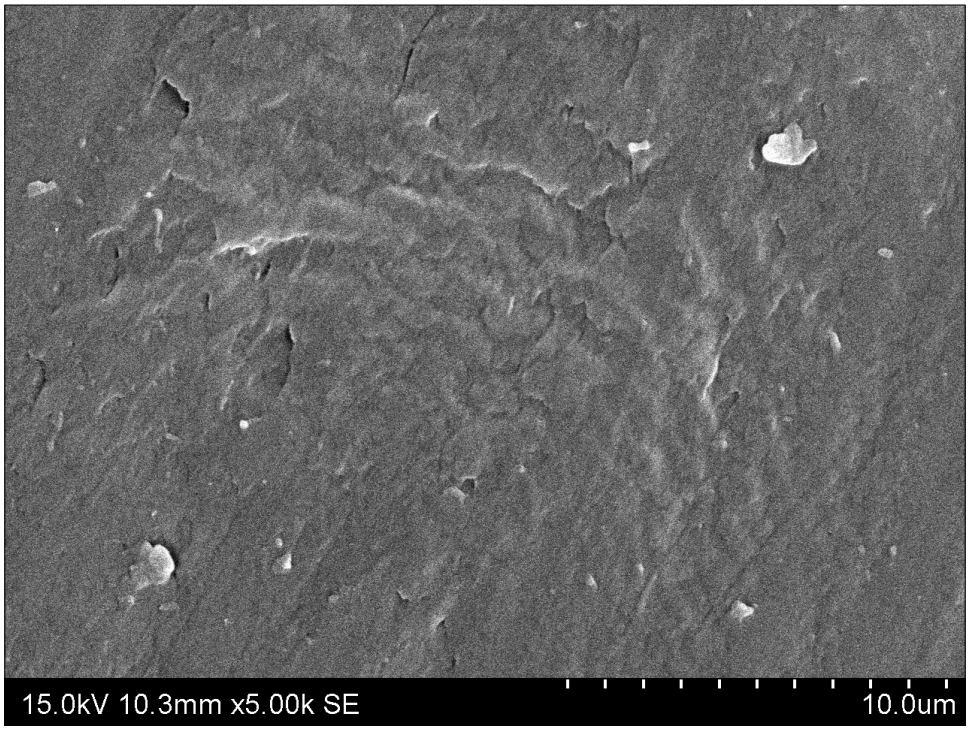

Figure S2: Polynorbornene (**PNBE**) with 10 wt% TiO_2

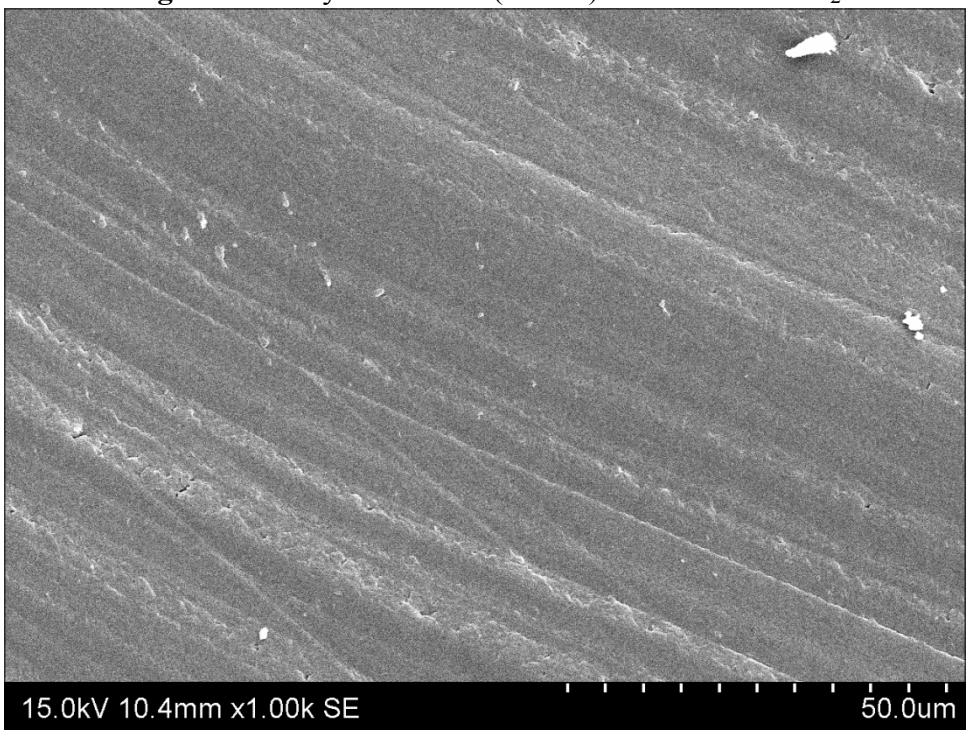

Figure S3: Polynorbornene (**PNBE**) with 20 wt% TiO_2

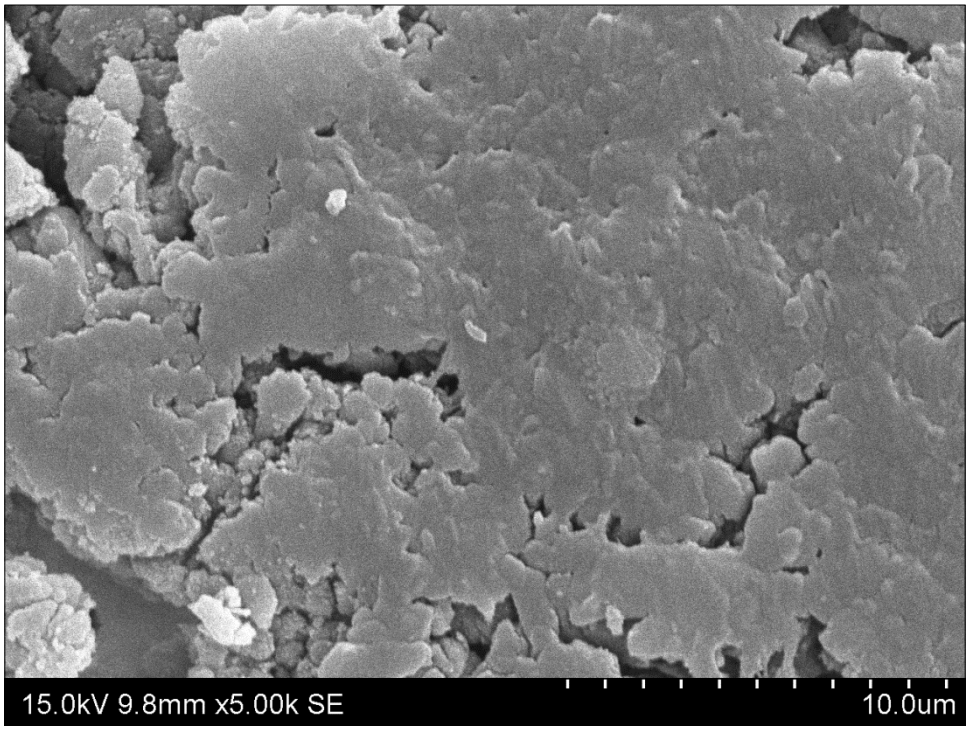

Figure S4: Polynorbornene (**PNBE**) with 50 wt% TiO_2

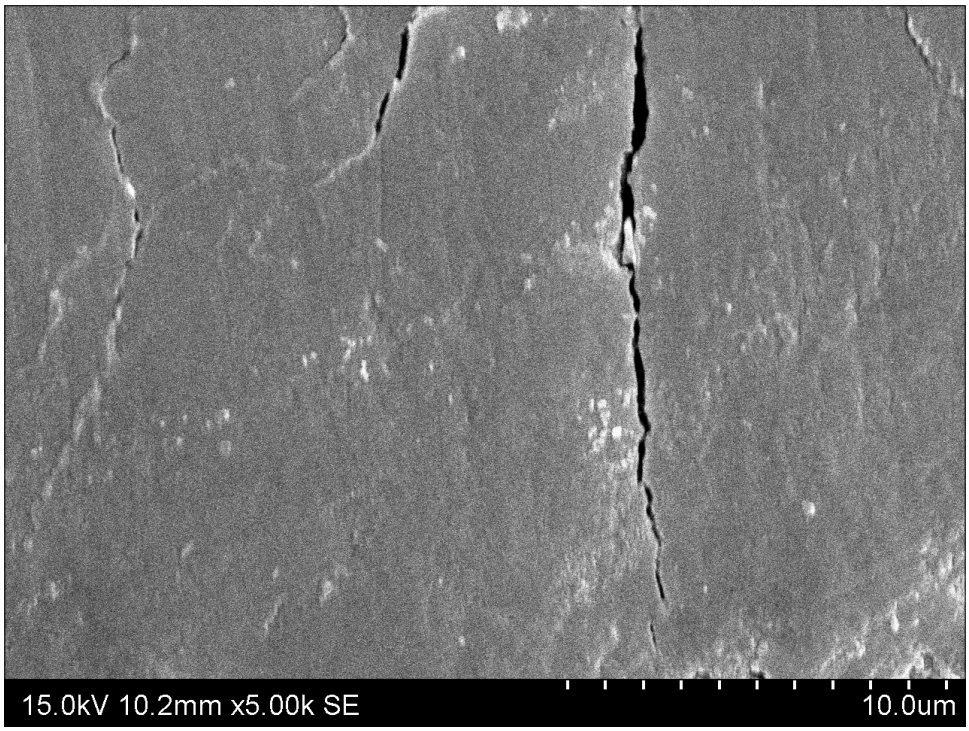

Figure S5: Polynorbornene (**PNBE**) with 10 wt% TiO_2 & AcAc

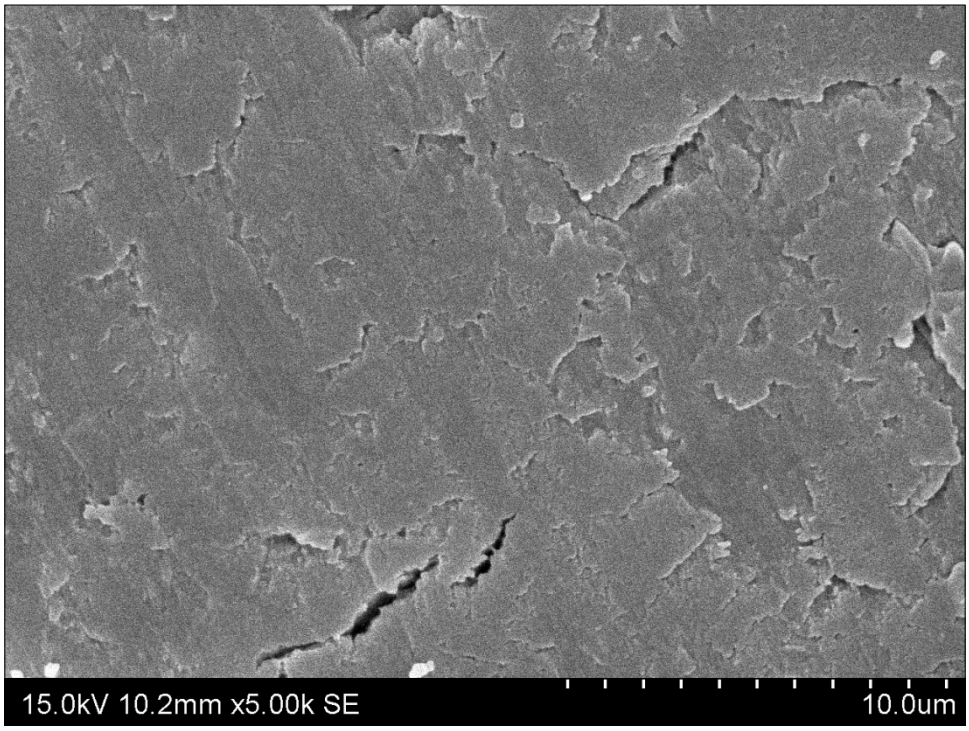

Figure S6: Polynorbornene (**PNBE**) with 20 wt% TiO_2 & AcAc

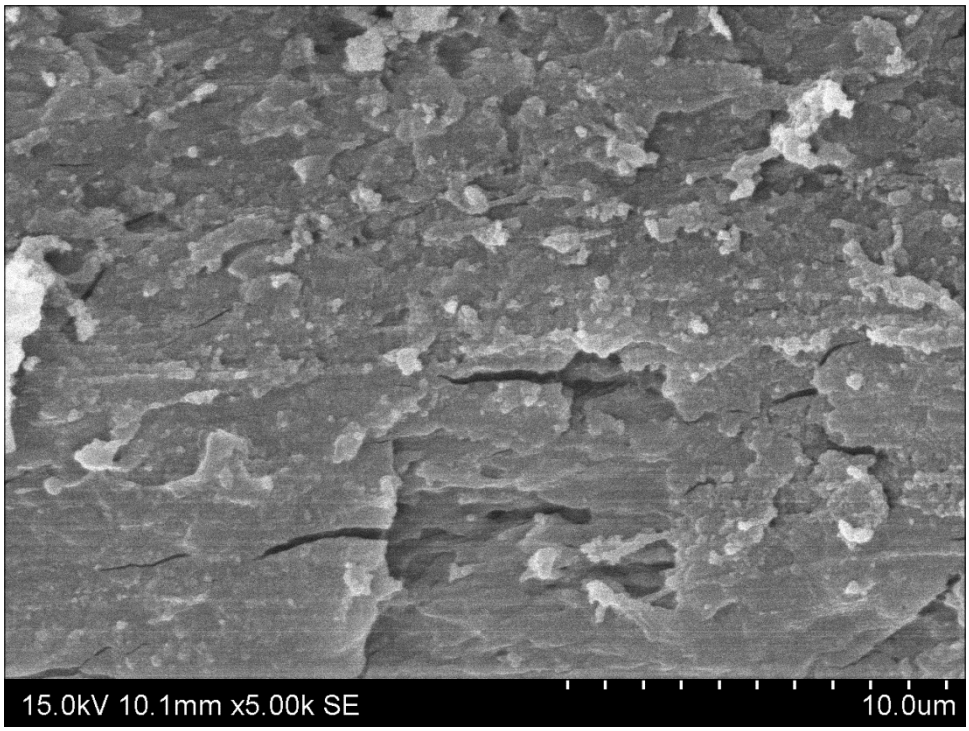

Figure S7: Polynorbornene (**PNBE**) with 50 wt% TiO_2 & AcAc

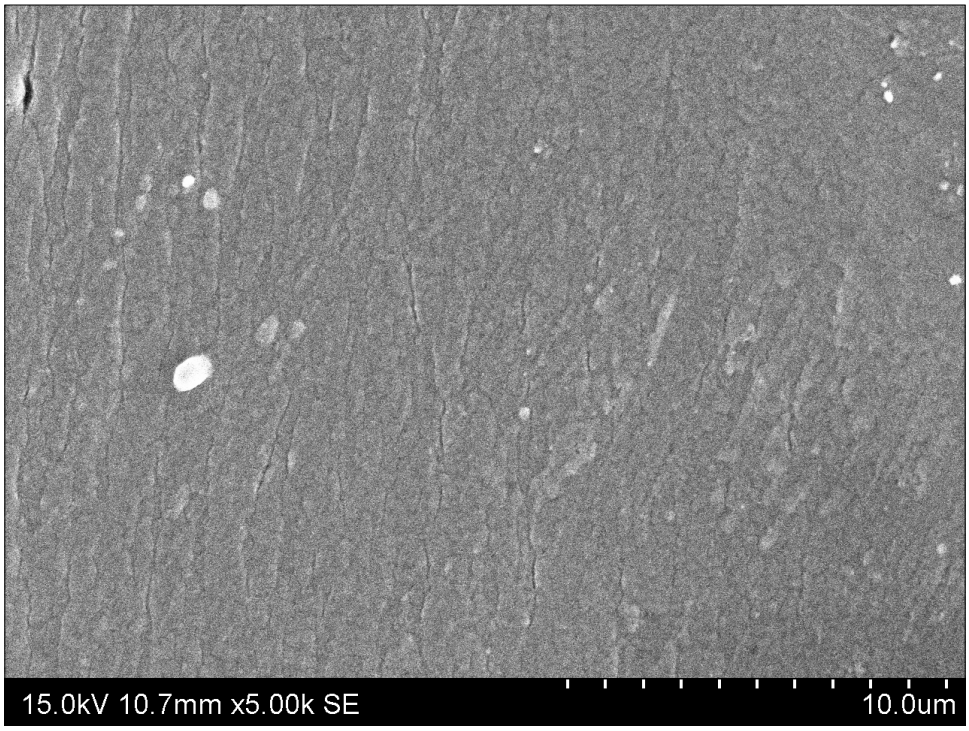

Figure S8: Poly((3aR,7aS)-2-butyl-3a,4,7,7a-tetrahydro-1H-4,7-epoxyisoindole-1,3(2H)-dione) poly(**M1**) with 10 wt% TiO_2 & AcAc

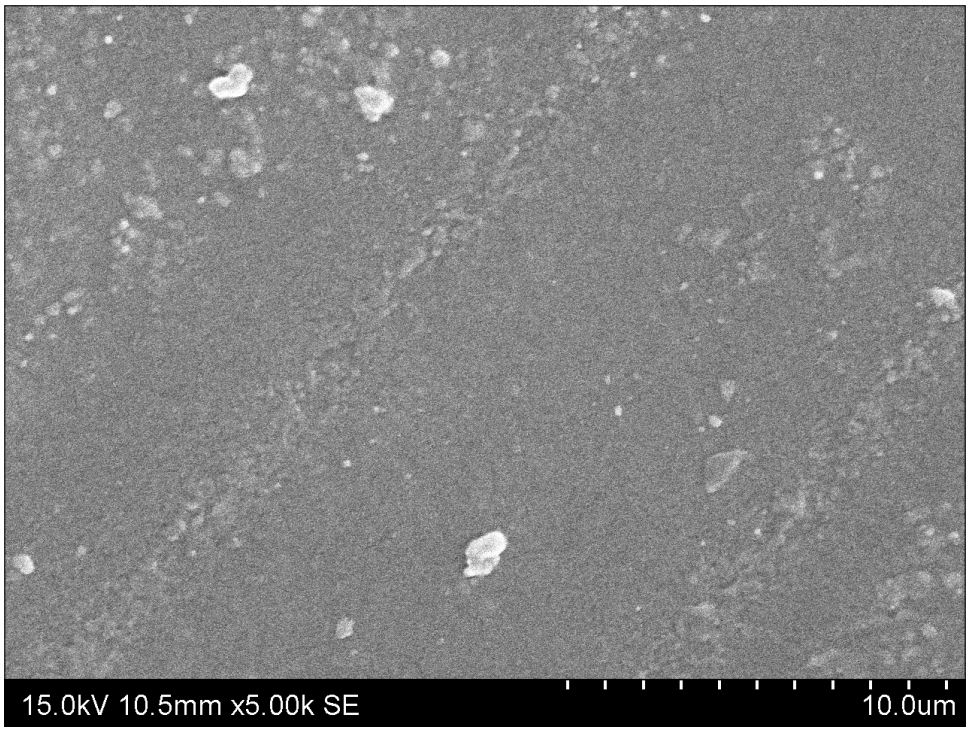

Figure S8: Poly((3aR,7aS)-2-butyl-3a,4,7,7a-tetrahydro-1H-4,7-epoxyisoindole-1,3(2H)-dione$_{80}$-*co*-2-((3aR,7aS)-1,3-dioxo-3a,4,7,7a-tetrahydro-1H-4,7-epoxyisoindol-2(3H)-yl)ethyl

3-((3-(triethoxysilyl)propyl)thio)propanoate$_{20}$) Poly(**M1**$_{80}$-*co*-**TES**$_{20}$) with 10 wt% TiO_2 & AcAc

1.2 HF etched hybrids and polymers

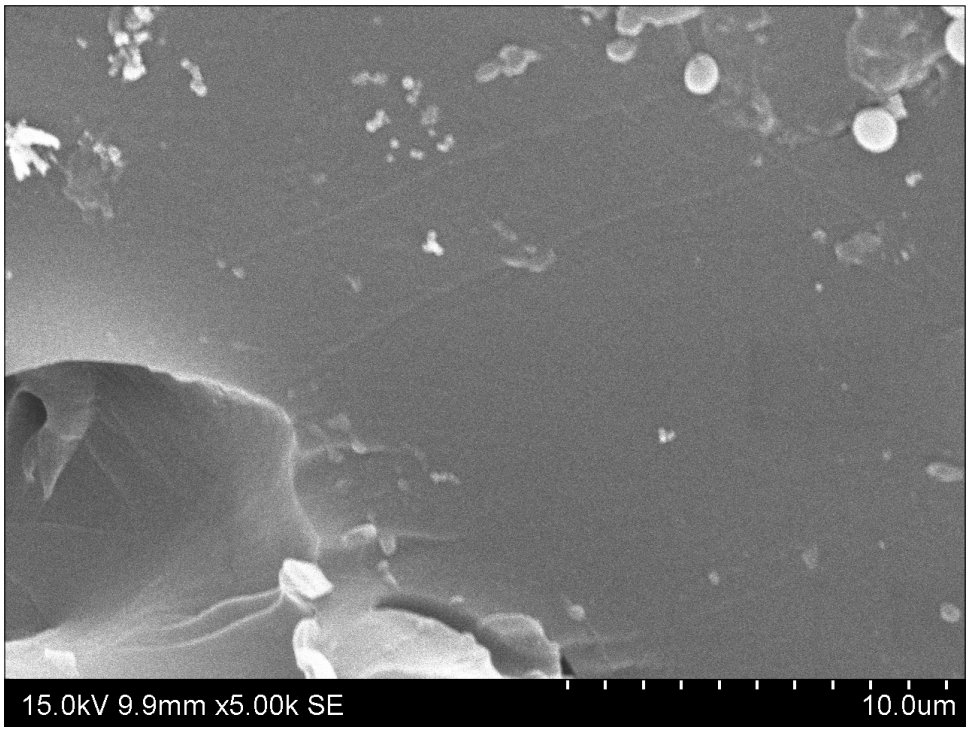

Figure S10: HF etched polynorbornene (**PNBE**)

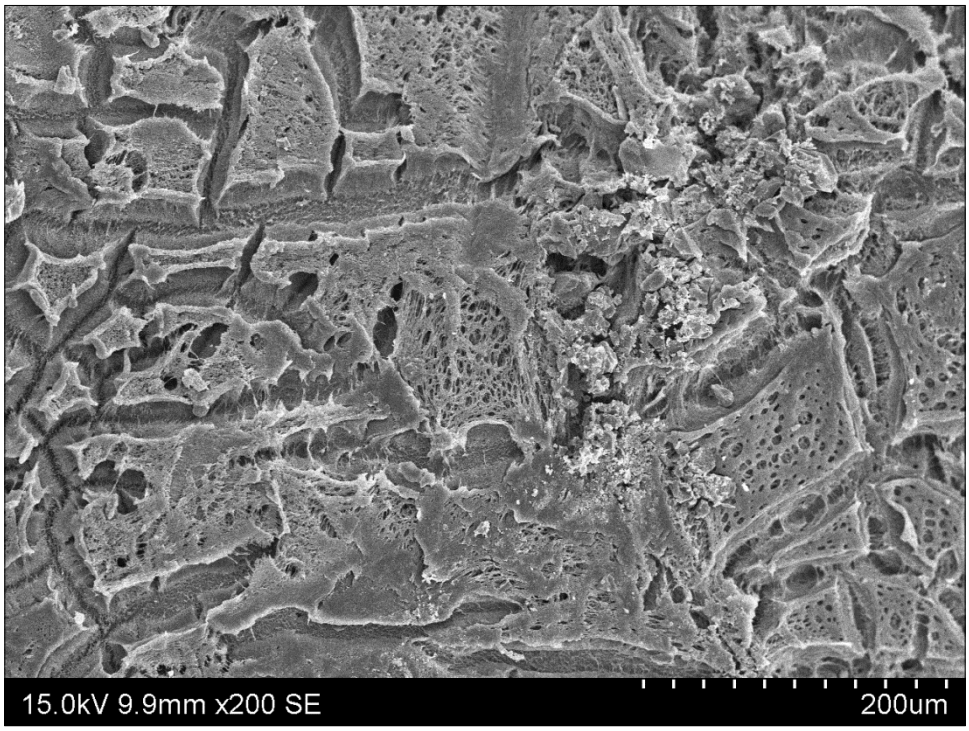

Figure S11: HF etched polynorbornene (**PNBE**) with 10 wt% TiO_2

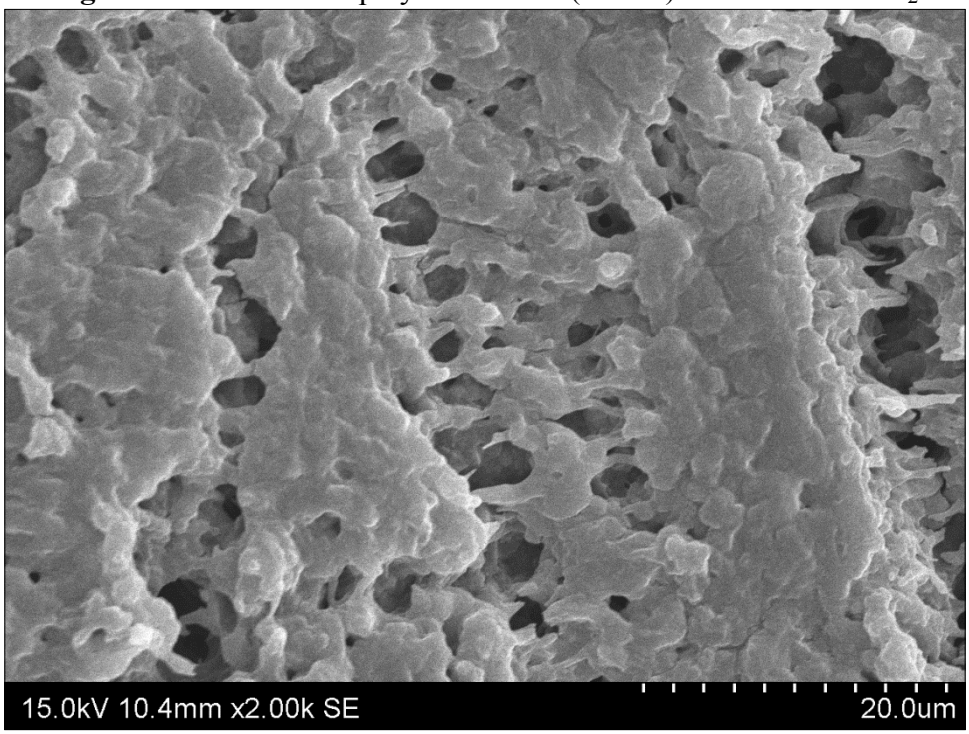

Figure S12: HF etched polynorbornene (**PNBE**) with 20 wt% TiO_2

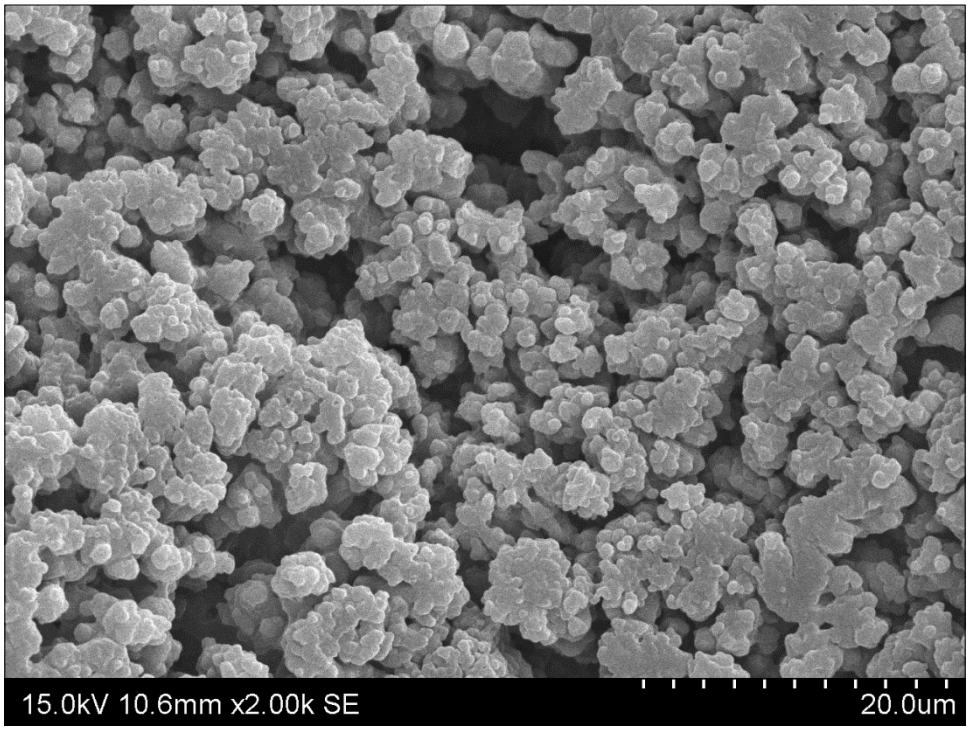

Figure S13: HF etched polynorbornene (**PNBE**) with 50 wt% TiO_2

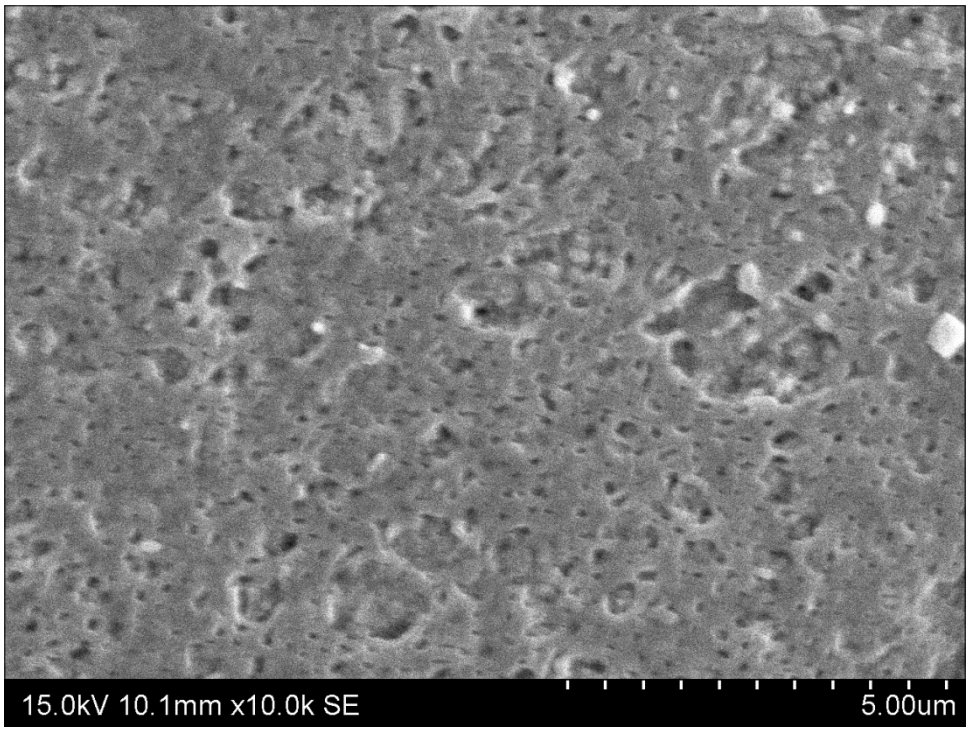

Figure S14: HF etched polynorbornene (**PNBE**) with 10 wt% TiO_2 & AcAc

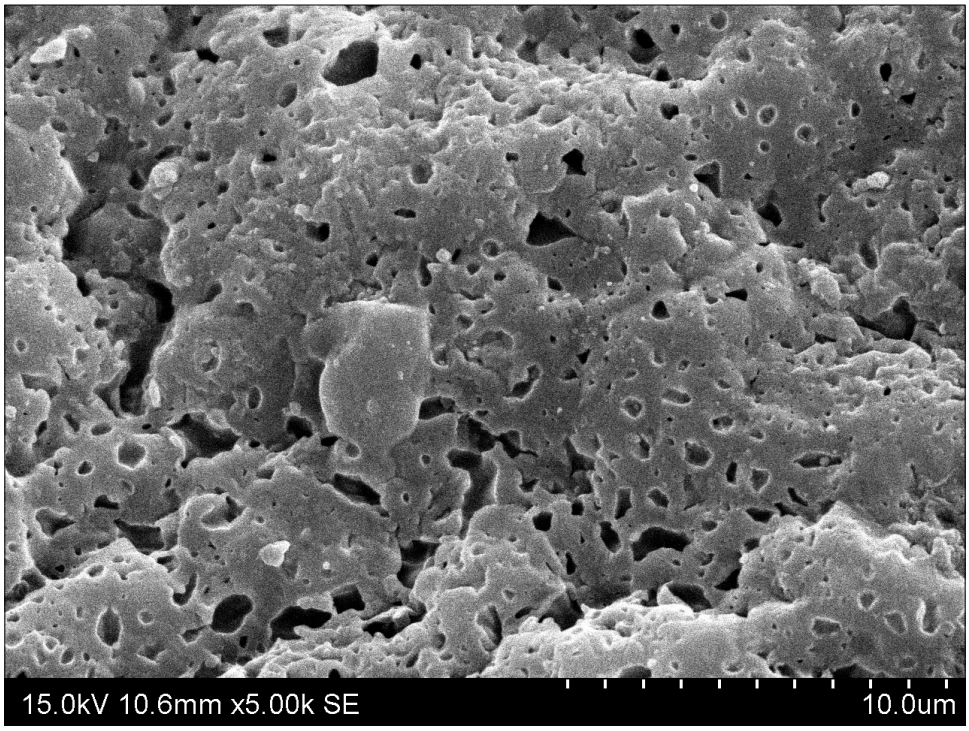

Figure S15: HF etched polynorbornene (**PNBE**) with 20 wt% TiO_2 & AcAc

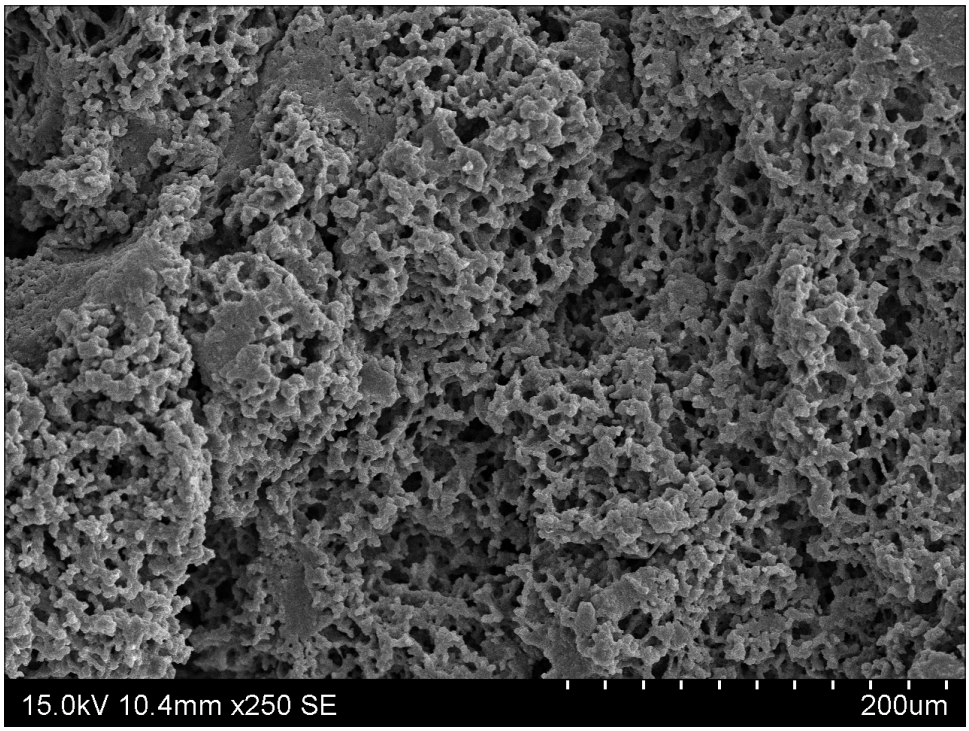

Figure S16: HF etched polynorbornene (**PNBE**) with 50 wt% TiO_2 & AcAc

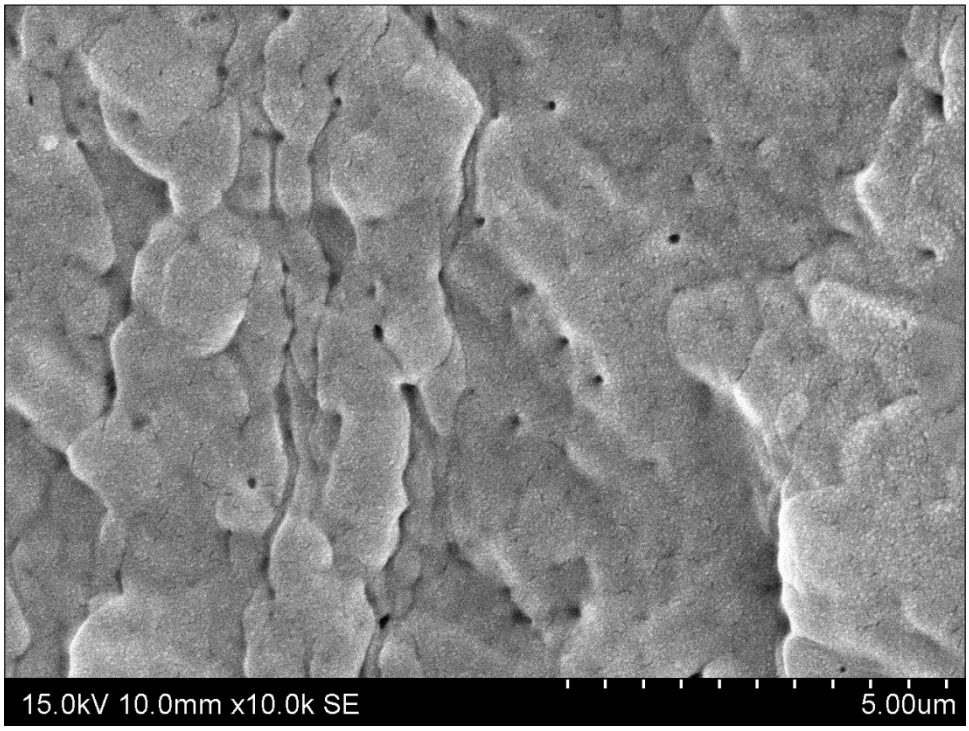

Figure S17: HF etched Poly((3aR,7aS)-2-butyl-3a,4,7,7a-tetrahydro-1H-4,7-epoxyisoindole-1,3(2H)-dione) poly(**M1**) with 10 wt% TiO_2 & AcAc

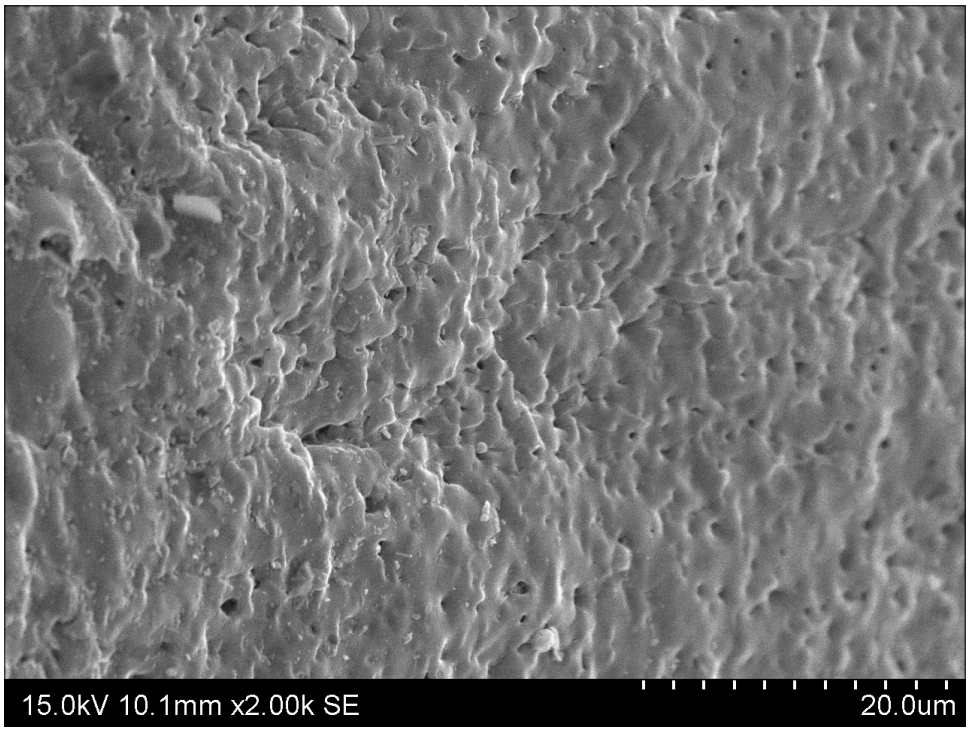

Figure S18: HF etched poly((3aR,7aS)-2-butyl-3a,4,7,7a-tetrahydro-1H-4,7-epoxyisoindole-1,3(2H)-dione$_{80}$-*co*-2-((3aR,7aS)-1,3-dioxo-3a,4,7,7a-tetrahydro-1H-4,7-epoxyisoindol-

2(3H)-yl)ethyl 3-((3-(triethoxysilyl)propyl)thio)propanoate$_{20}$) Poly(**M1**$_{80}$-*co*-**TES**$_{20}$) with 10 wt% TiO_2 & AcAc

1.3 Pyrolysis chars

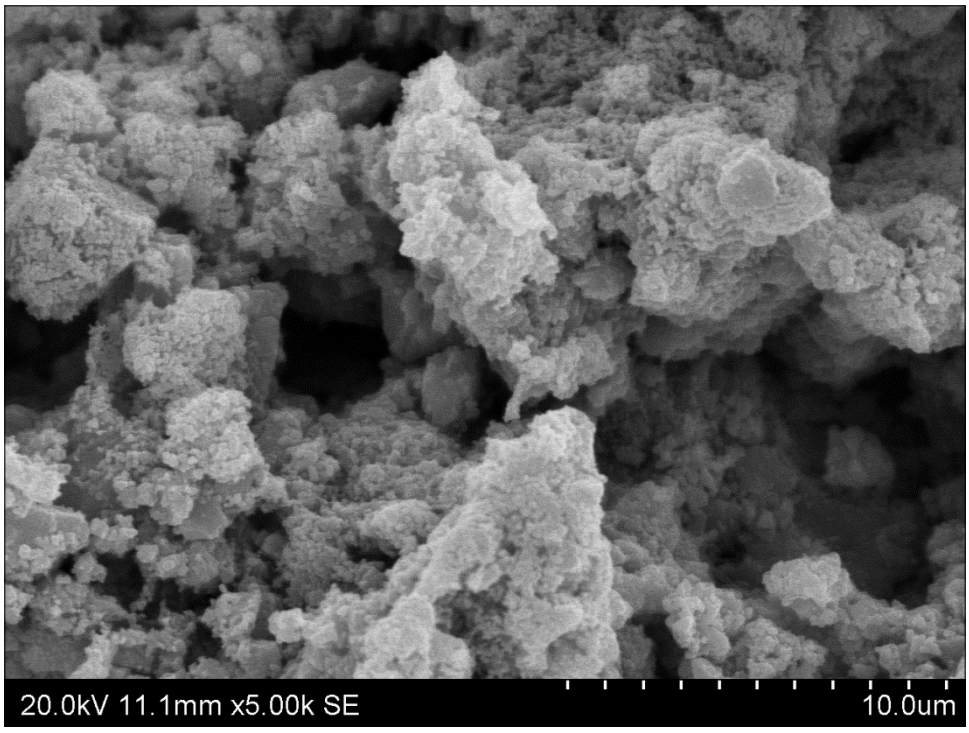

Figure S19: Pyrolysis char of polynorbornene (**PNBE**) with 10 wt% TiO_2

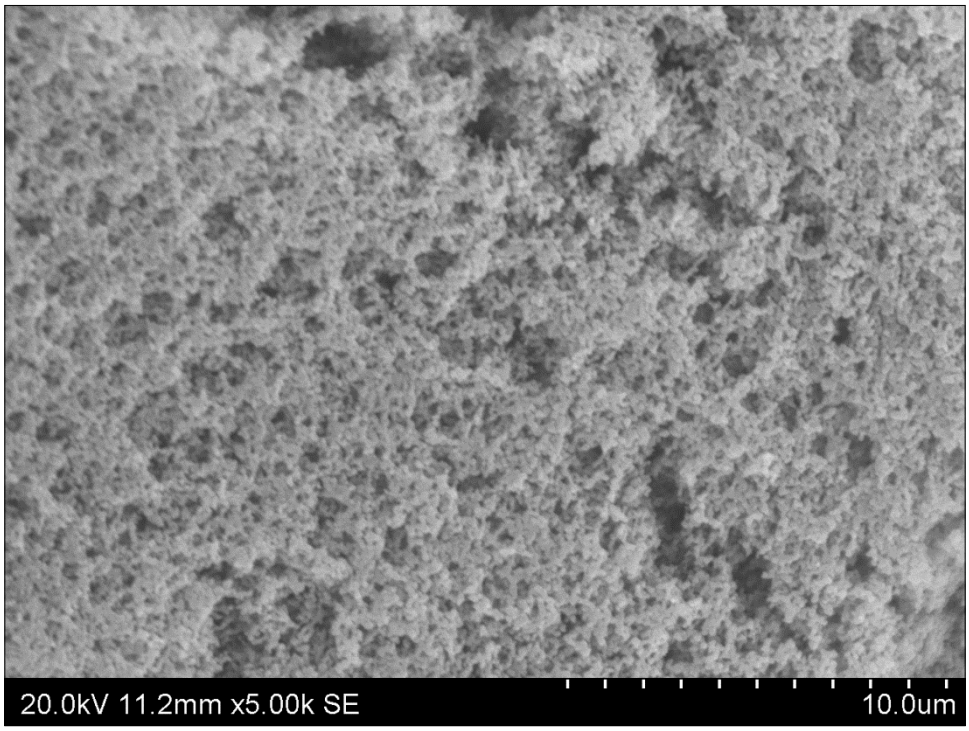

Figure S20: Pyrolysis char of polynorbornene (**PNBE**) with 20 wt% TiO_2

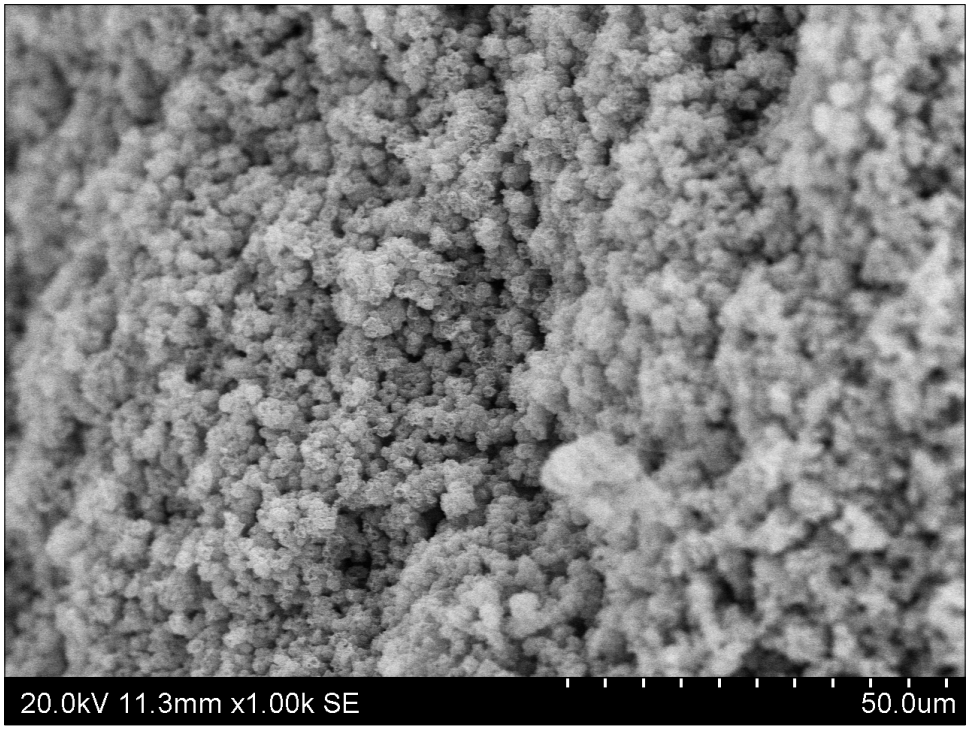

Figure S21: Pyrolysis char of polynorbornene (**PNBE**) with 50 wt% TiO_2

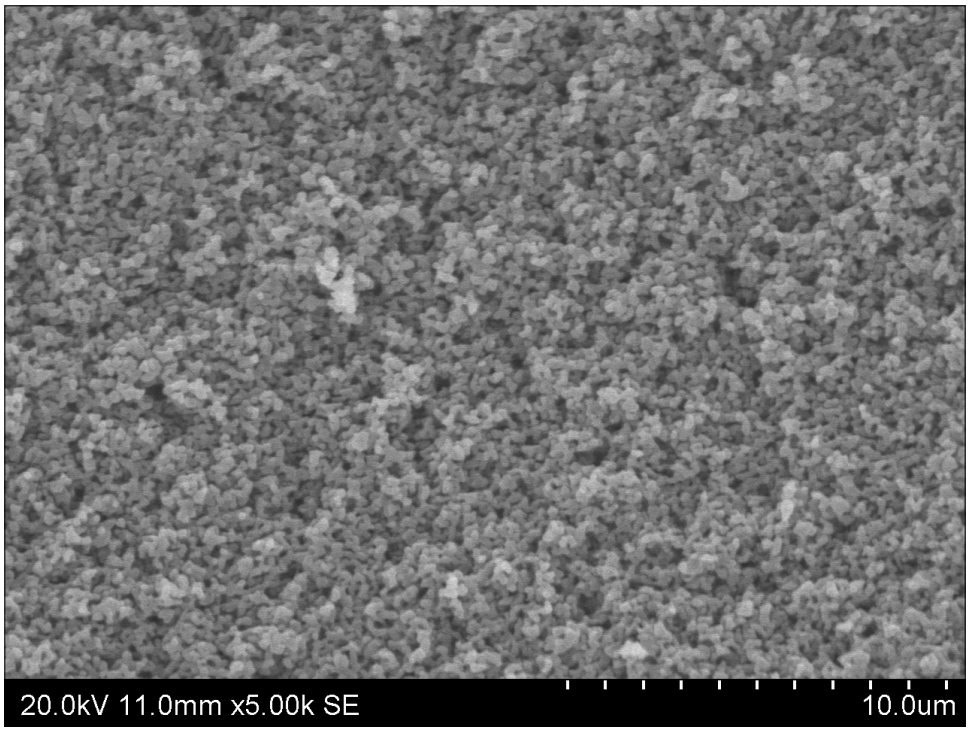

Figure S22: Pyrolysis char of polynorbornene (**PNBE**) with 10 wt% TiO_2 & AcAc

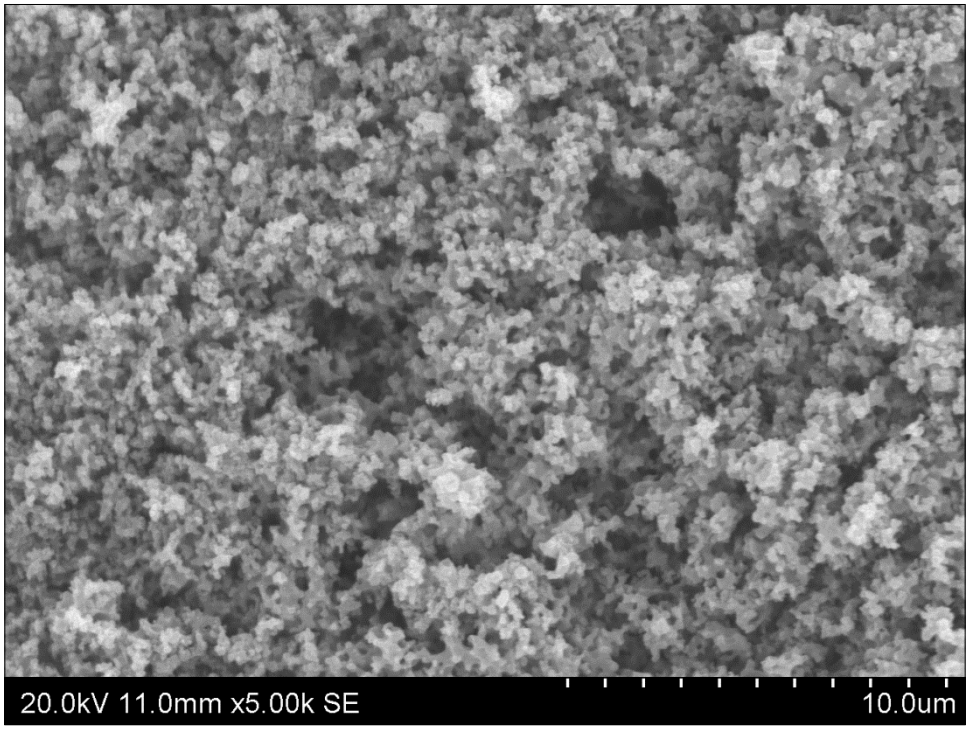

Figure S23: Pyrolysis char of polynorbornene (**PNBE**) with 20 wt% TiO_2 & AcAc

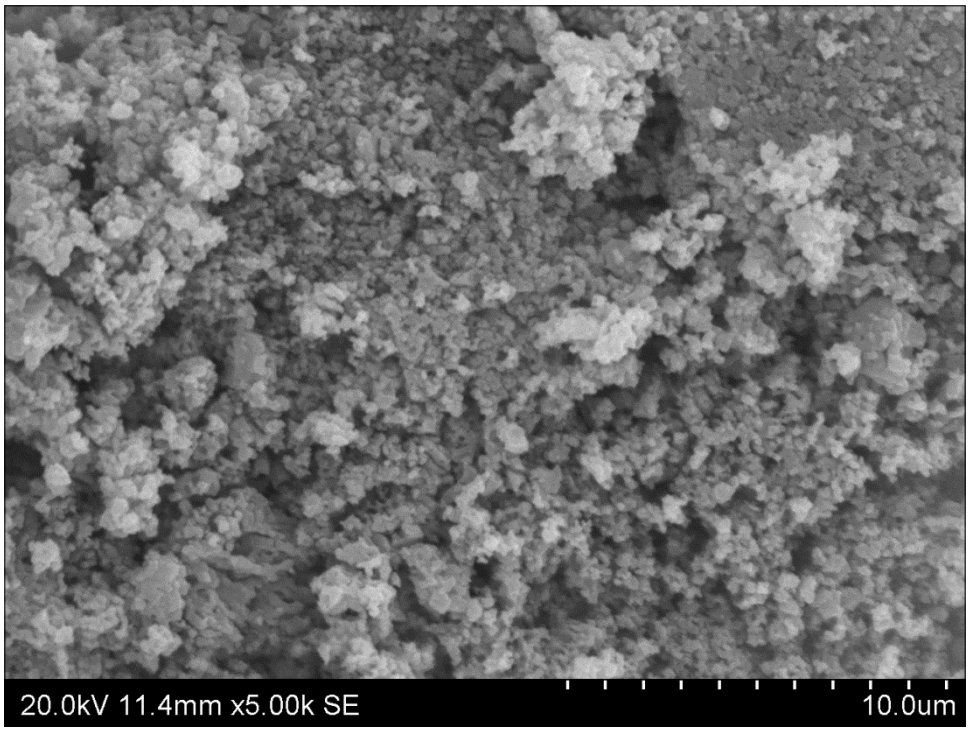

Figure S24: Pyrolysis char of polynorbornene (**PNBE**) with 50 wt% TiO_2 & AcAc

2. Additional TEM images

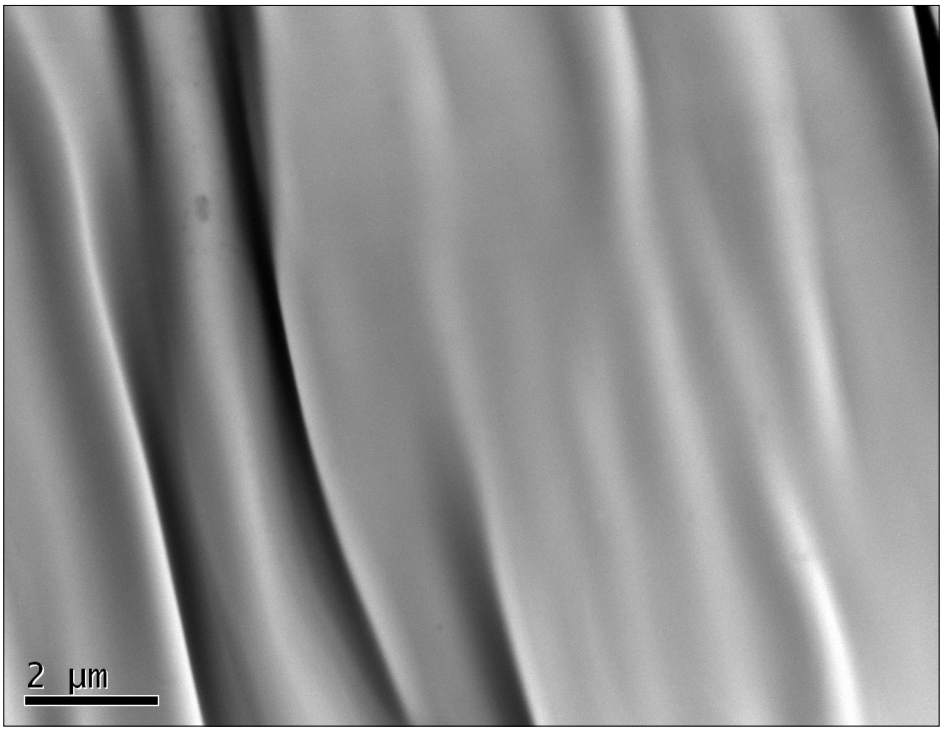

Figure S25: Polynorbornene (**PNBE**)

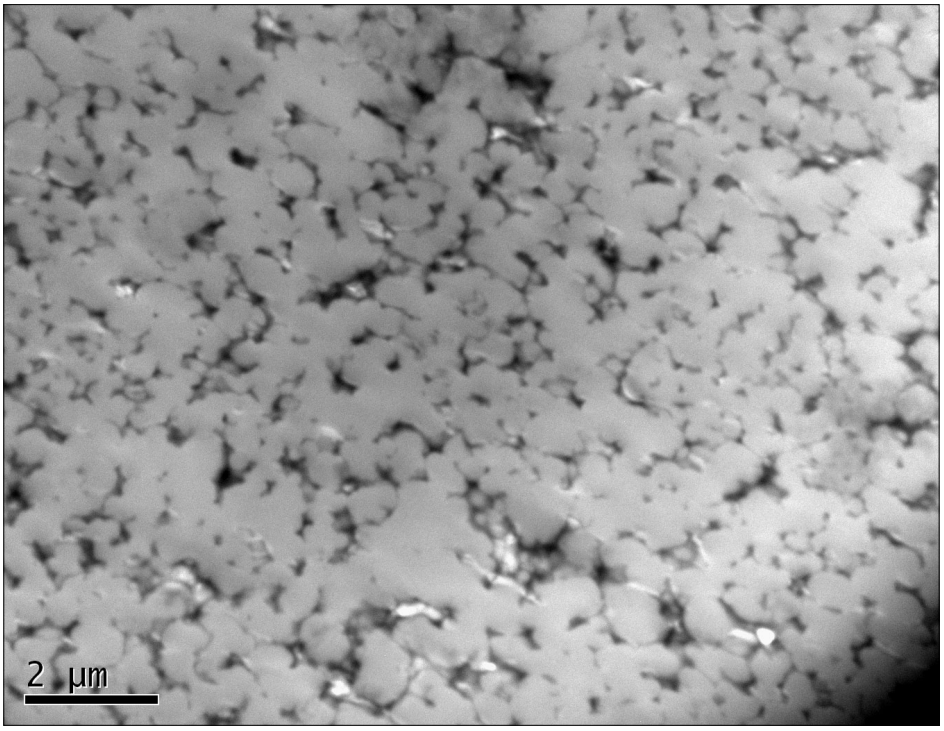

Figure S26: Polynorbornene (**PNBE**) with 10 wt% TiO_2

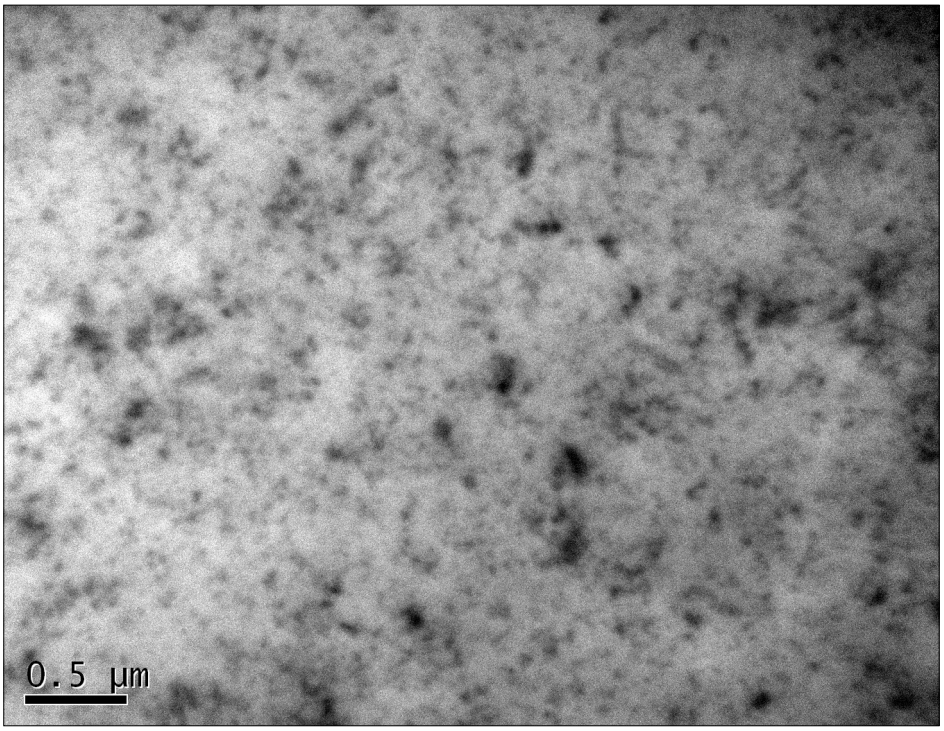

Figure S27: Polynorbornene (**PNBE**) with 10 wt% TiO_2 & AcAc

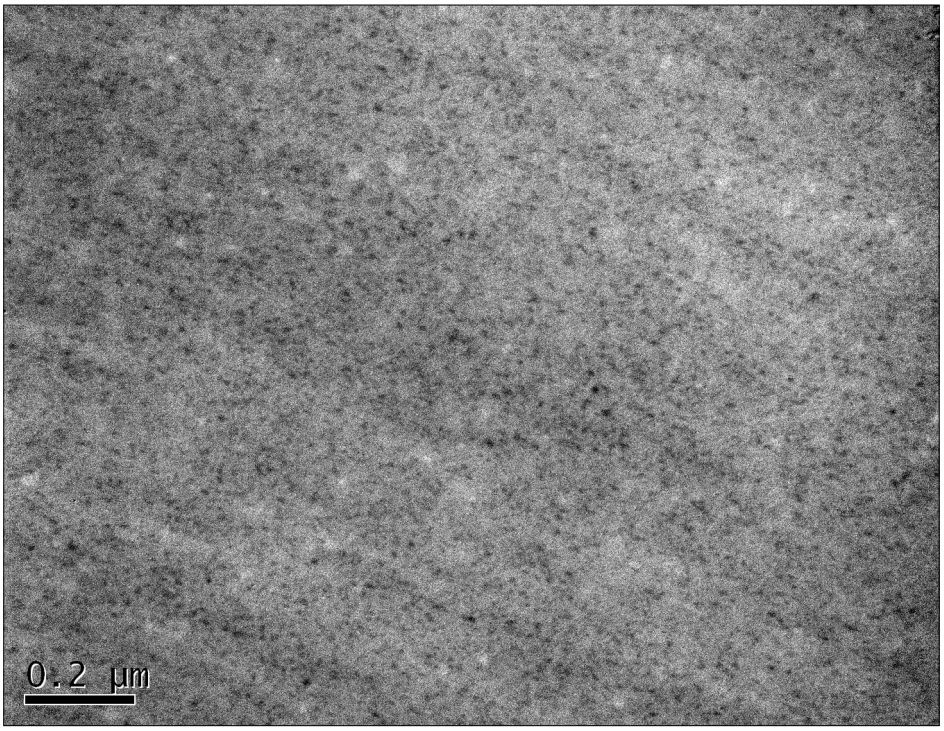

Figure S28: Poly((3aR,7aS)-2-butyl-3a,4,7,7a-tetrahydro-1H-4,7-epoxyisoindole-1,3(2H)-dione) poly(**M1**) with 10 wt% TiO_2 & AcAc

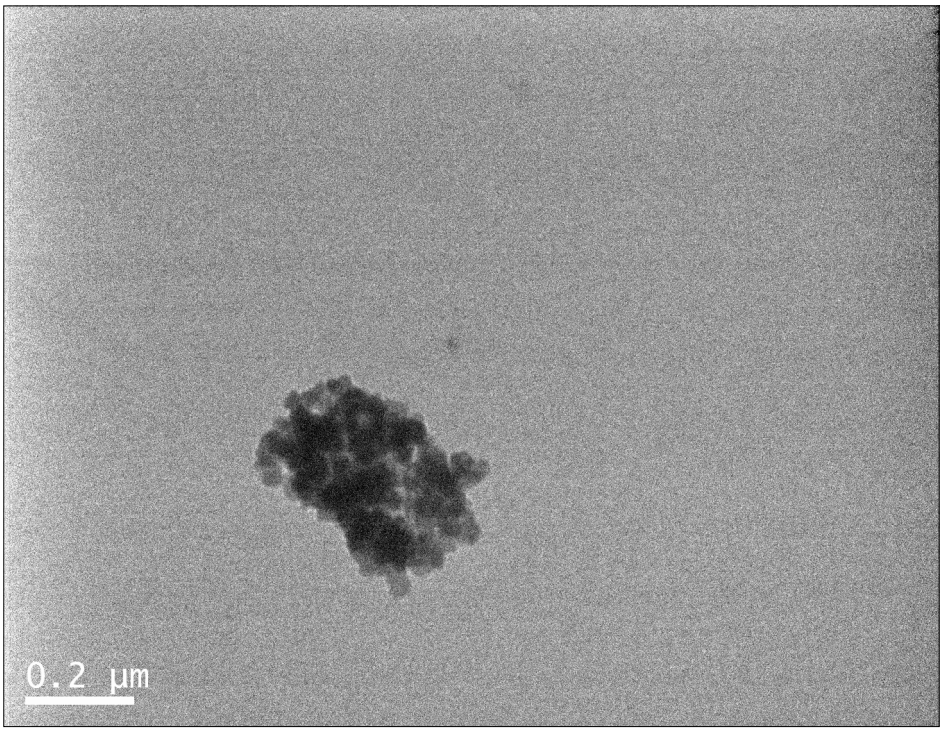

Figure S29: Poly(2-((3aR,7aS)-1,3-dioxo-3a,4,7,7a-tetrahydro-1H-4,7-epoxyisoindol-2(3H)-yl)ethyl 3-((3-(triethoxysilyl)propyl)thio)propanoate) poly(**TES**) with 10 wt% TiO_2 & AcAc

NB: Includes artifact to verify focus

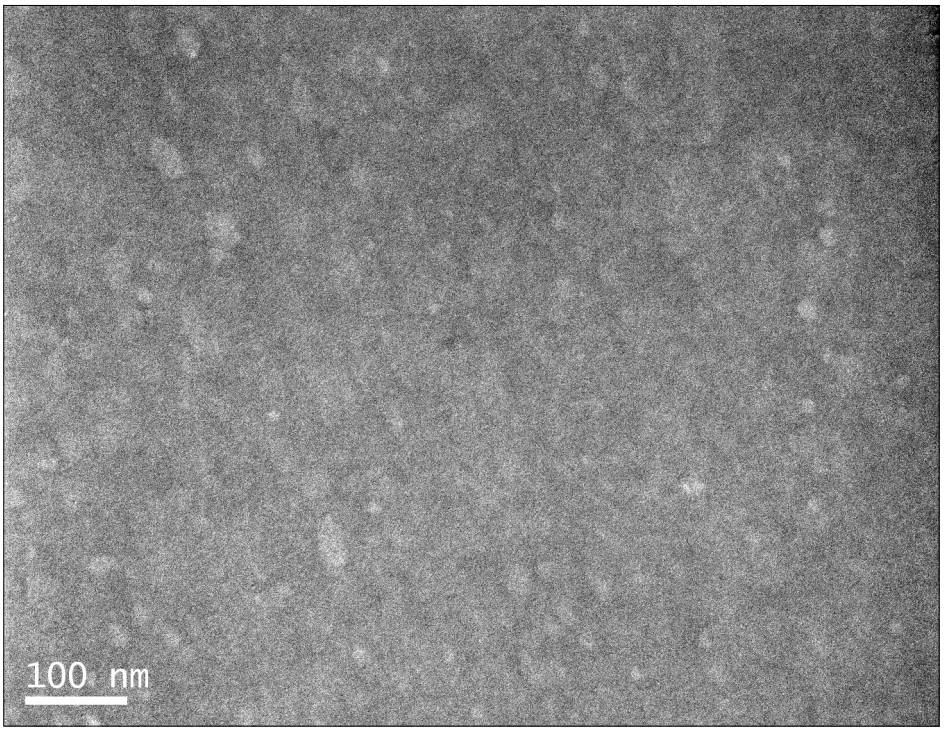

Figure S30: Poly(2-((3aR,7aS)-1,3-dioxo-3a,4,7,7a-tetrahydro-1H-4,7-epoxyisoindol-2(3H)-yl)ethyl 3-((3-(triethoxysilyl)propyl)thio)propanoate) poly(**TES**) with 30 wt% TiO_2 & AcAc

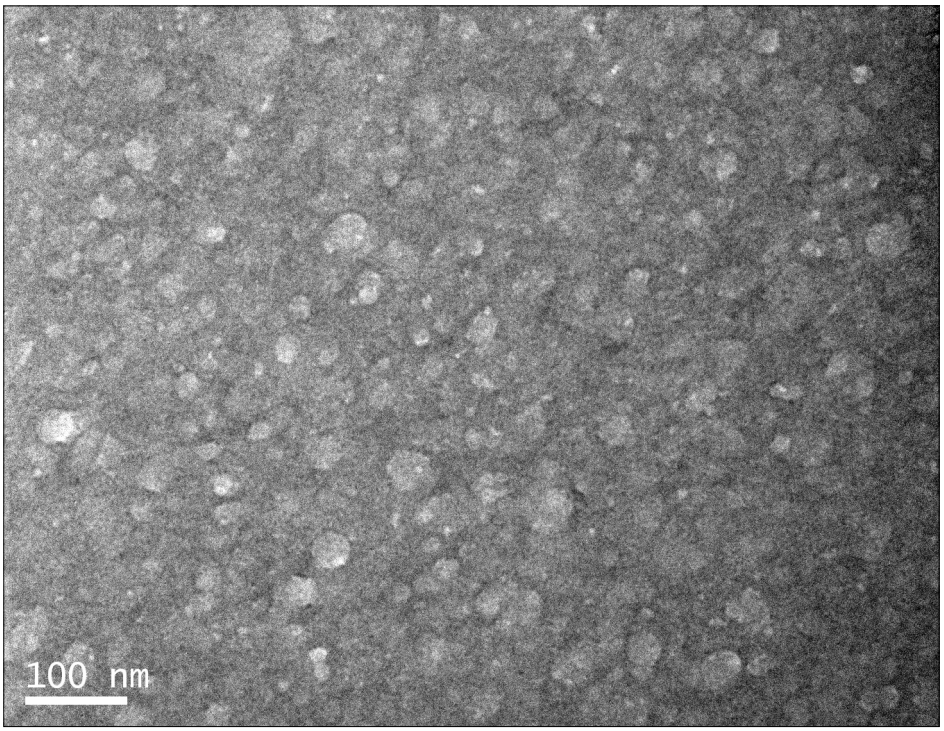

Figure S31: Poly(2-((3aR,7aS)-1,3-dioxo-3a,4,7,7a-tetrahydro-1H-4,7-epoxyisoindol-2(3H)-yl)ethyl 3-((3-(triethoxysilyl)propyl)thio)propanoate) poly(**TES**) with 50 wt% TiO_2 & AcAc

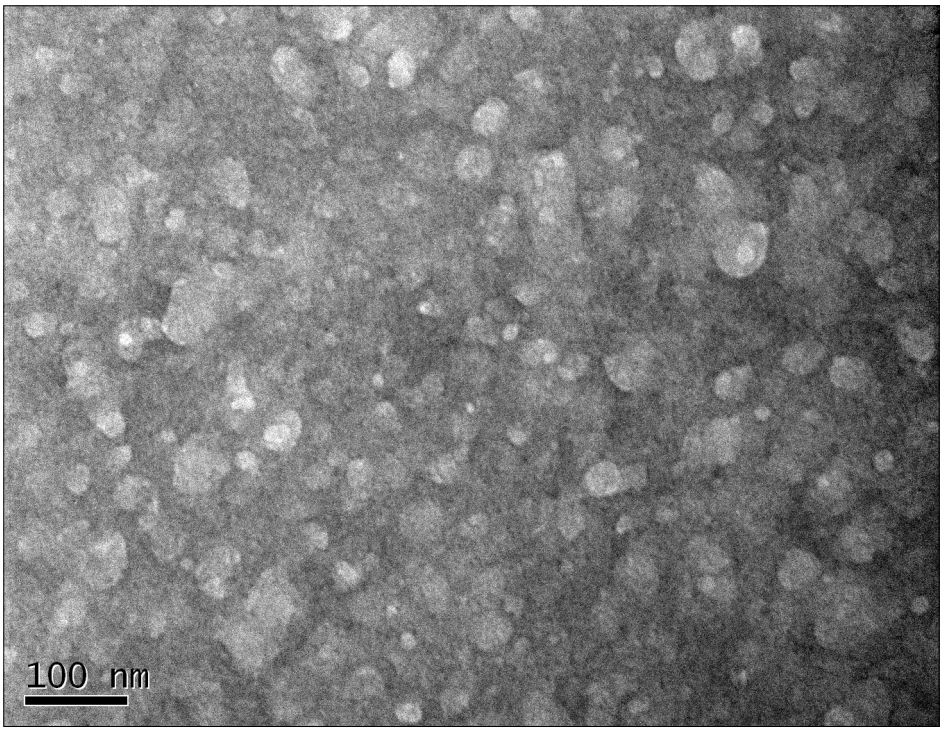

Figure S32: Poly(norbornenylethylisobutyl POSS$^{(R)}{}_{50}$-*co*-2-((3a*R*,7a*S*)-1,3-dioxo-3a,4,7,7a-tetrahydro-1*H*-4,7-epoxyisoindol-2(3*H*)-yl)ethyl 3-((3-(triethoxysilyl)propyl) thio)propanoate$_{50}$) poly(**POSS1**$_{50}$-*co*-**TES**$_{50}$) with 50 wt% TiO_2 & AcAc

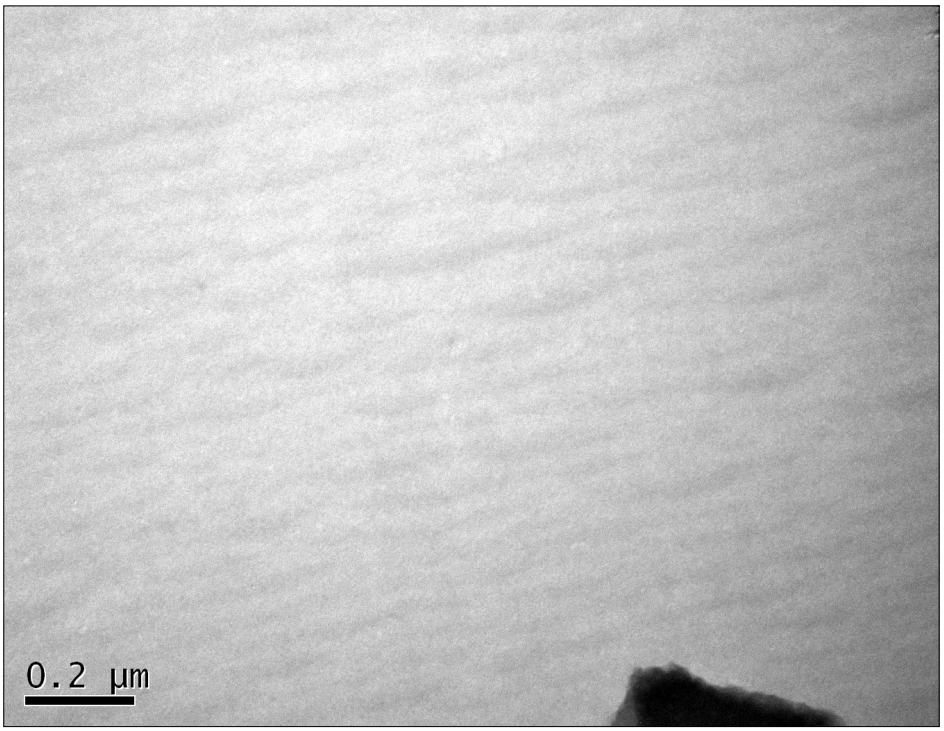

Figure S33: Poly((2S,3S,4S,5R,6R)-6-((3-(2-((3aR,7aS)-1,3-dioxo-1,3,3a,4,7,7a-hexahydro-2H-4,7-epoxyisoindol-2-yl)ethoxy)-3-oxopropyl)thio)tetrahydro-2H-pyran-2,3,4,5-

tetrayltetraacetate$_{50}$-*co*-2-((3a*R*,7a*S*)-1,3-dioxo-3a,4,7,7a-tetrahydro-1*H*-4,7-epoxyisoindol-2(3*H*)-yl)ethyl 3-((3-(triethoxysilyl)propyl) thio)propanoate$_{50}$) poly(**M5**$_{50}$-*co*-**TES**$_{50}$) with 50 wt% TiO_2 & AcAc
NB: Includes artifact to verify focus

3. Additional TGA traces

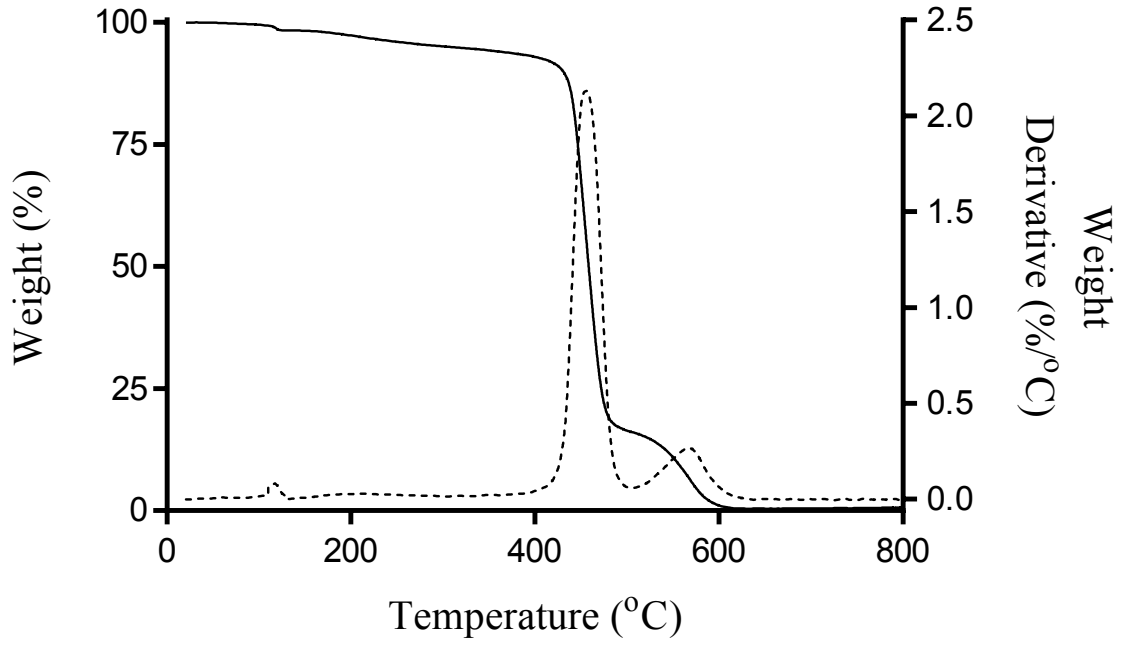

Figure S34: Polynorbornene (**PNBE**)

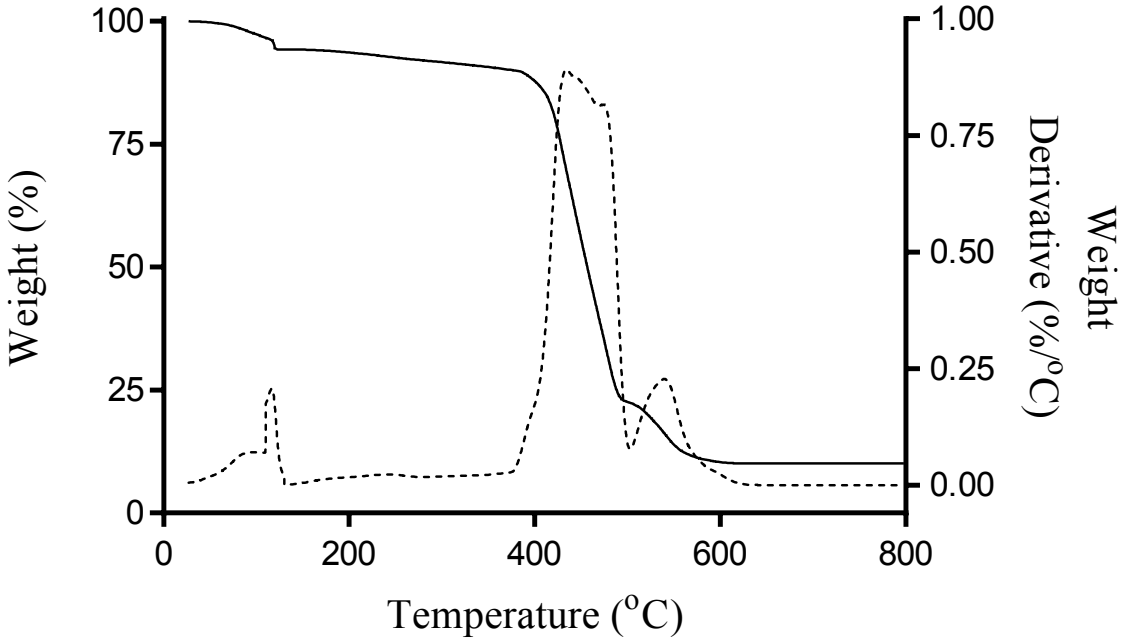

Figure S35: Polynorbornene (**PNBE**) with 10 wt% TiO_2

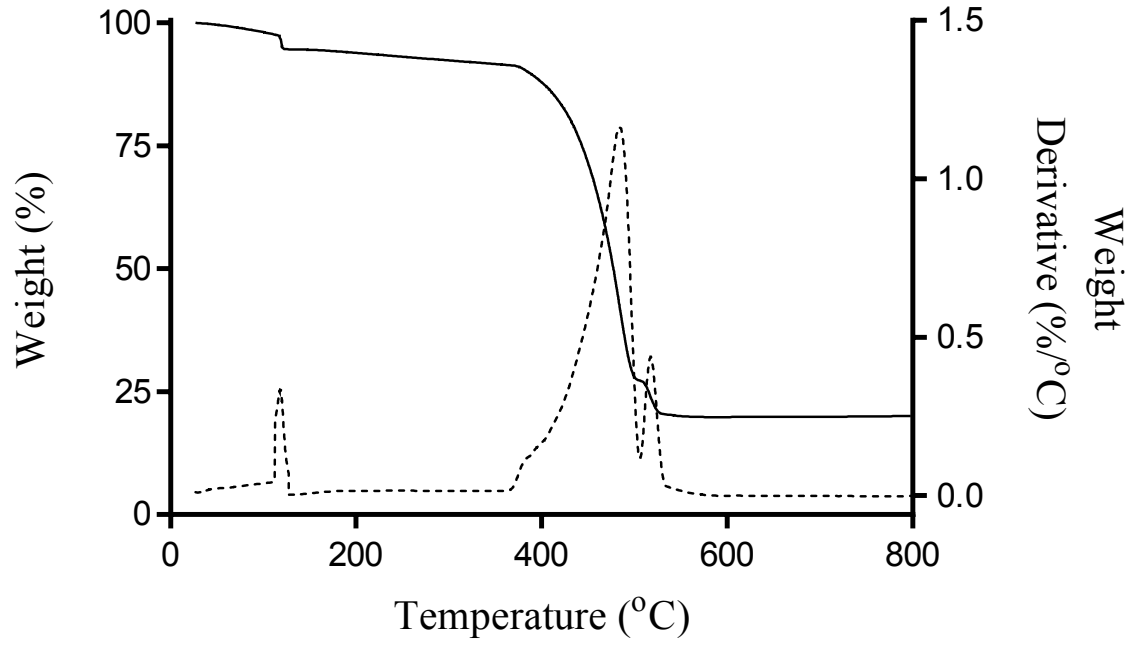

Figure S36: Polynorbornene (**PNBE**) with 20 wt% TiO_2

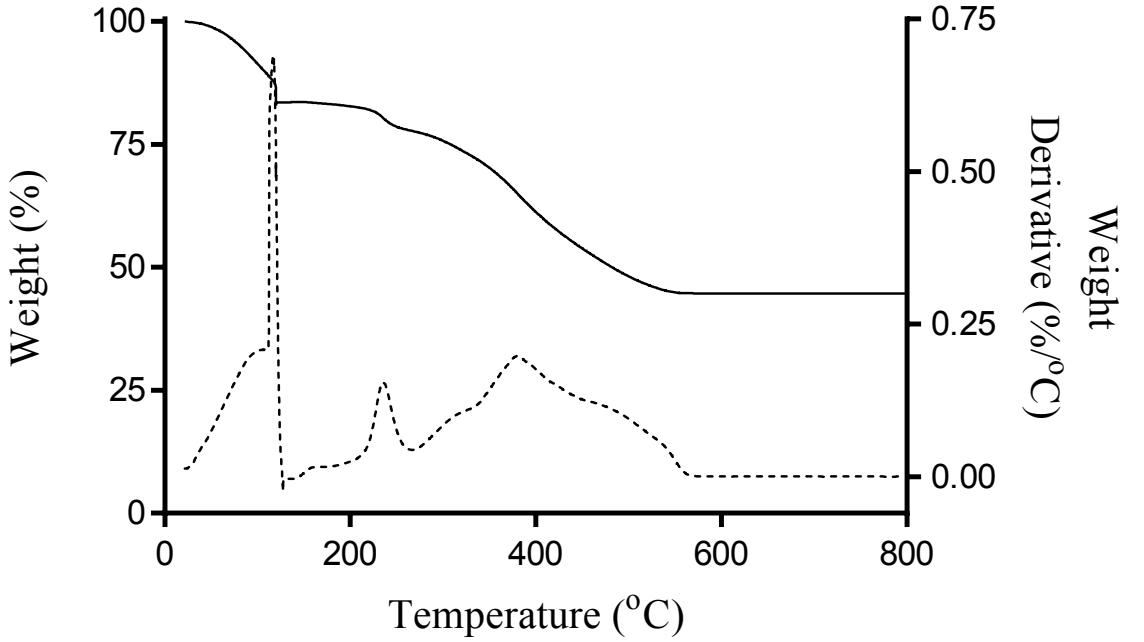

Figure S37: Polynorbornene (**PNBE**) with 50 wt% TiO_2

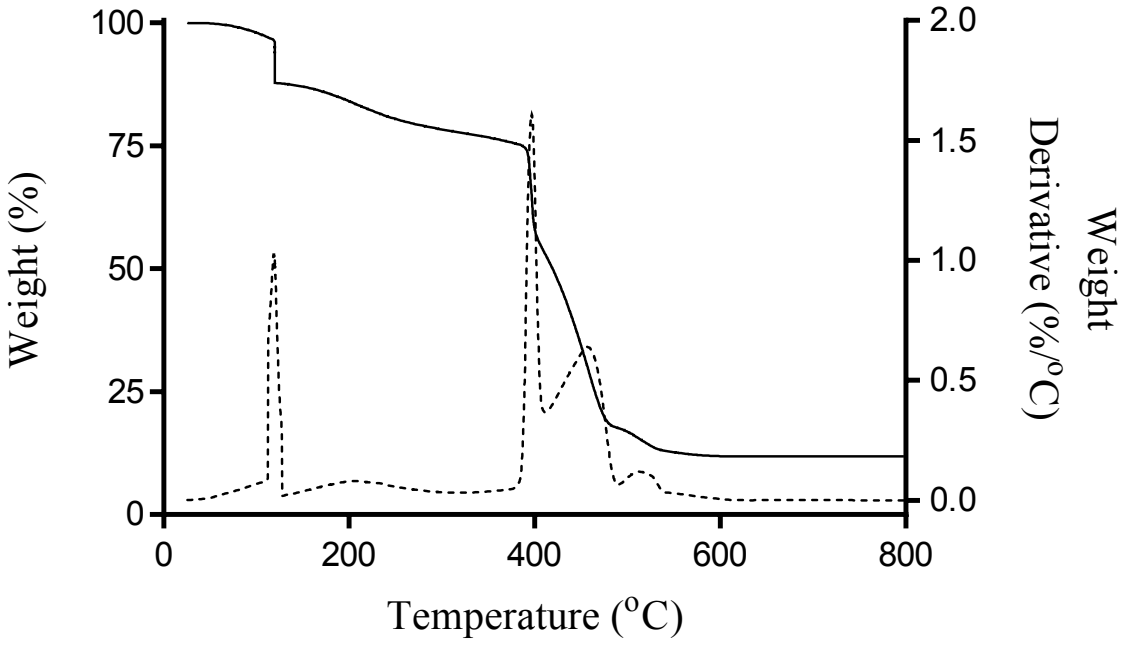

Figure S38: Polynorbornene (**PNBE**) with 10 wt% TiO_2 & AcAc

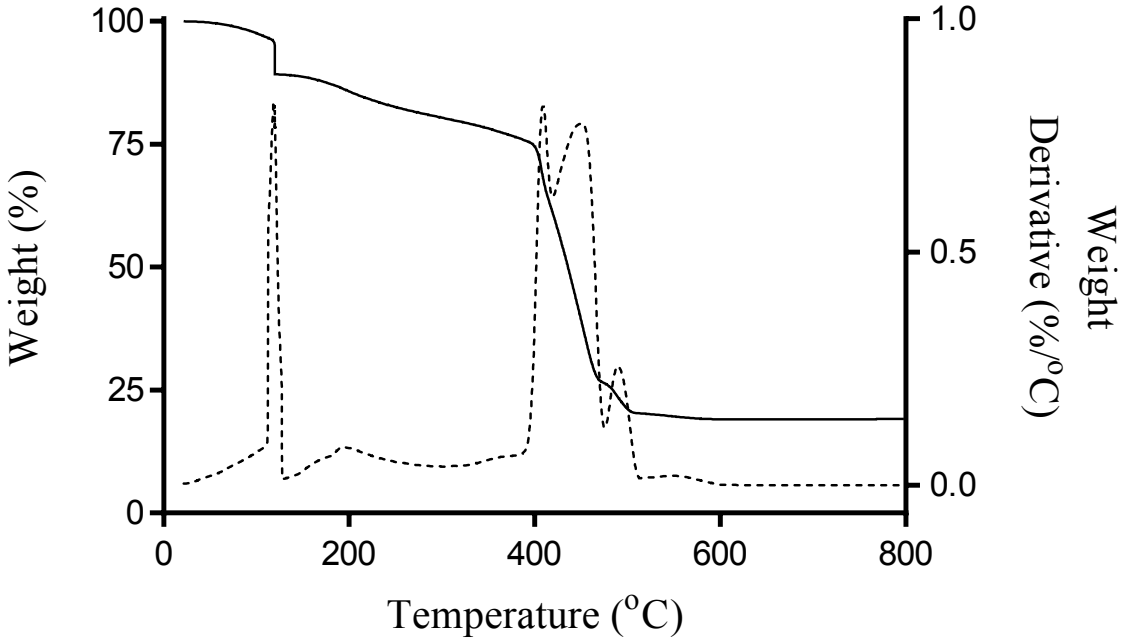

Figure S39: Polynorbornene (**PNBE**) with 20 wt% TiO_2 & AcAc

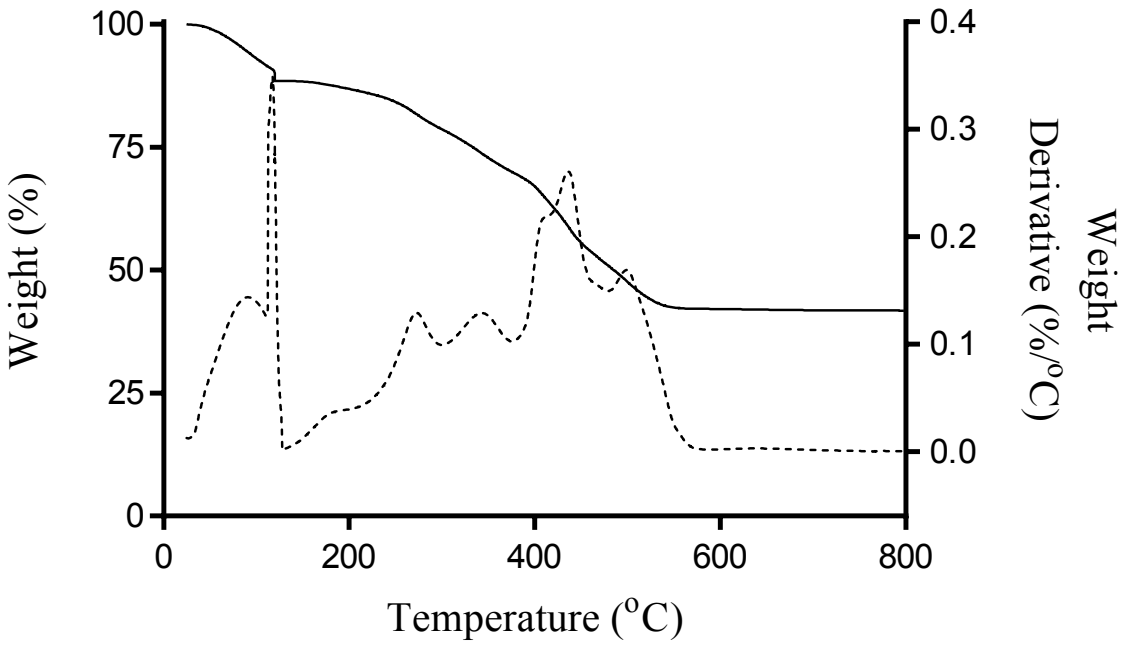

Figure S40: Polynorbornene (**PNBE**) with 50 wt% TiO_2 & AcAc

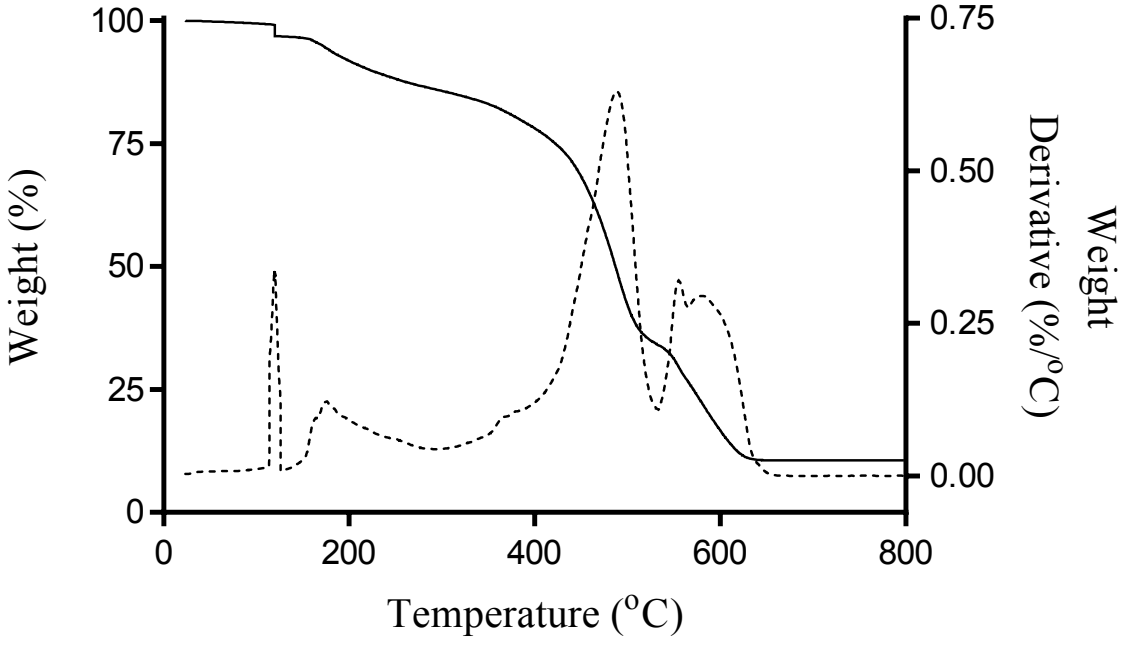

Figure S41: Poly((3aR,7aS)-2-butyl-3a,4,7,7a-tetrahydro-1H-4,7-epoxyisoindole-1,3(2H)-dione) poly(**M1**) with 10 wt% TiO_2 & AcAc

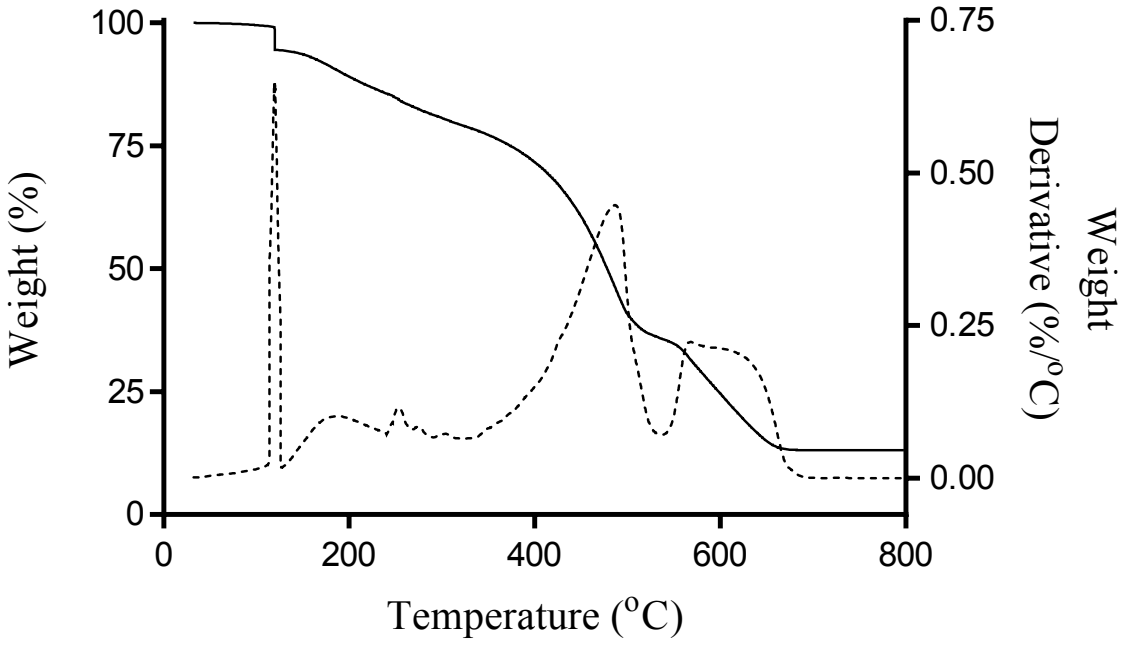

Figure S42: Poly((3aR,7aS)-2-butyl-3a,4,7,7a-tetrahydro-1H-4,7-epoxyisoindole-1,3(2H)-dione$_{80}$-*co*-2-((3aR,7aS)-1,3-dioxo-3a,4,7,7a-tetrahydro-1H-4,7-epoxyisoindol-2(3H)-yl)ethyl 3-((3-(triethoxysilyl)propyl)thio)propanoate$_{20}$) Poly(**M1**$_{80}$-*co*-**TES**$_{20}$) with 10 wt% TiO_2 & AcAc

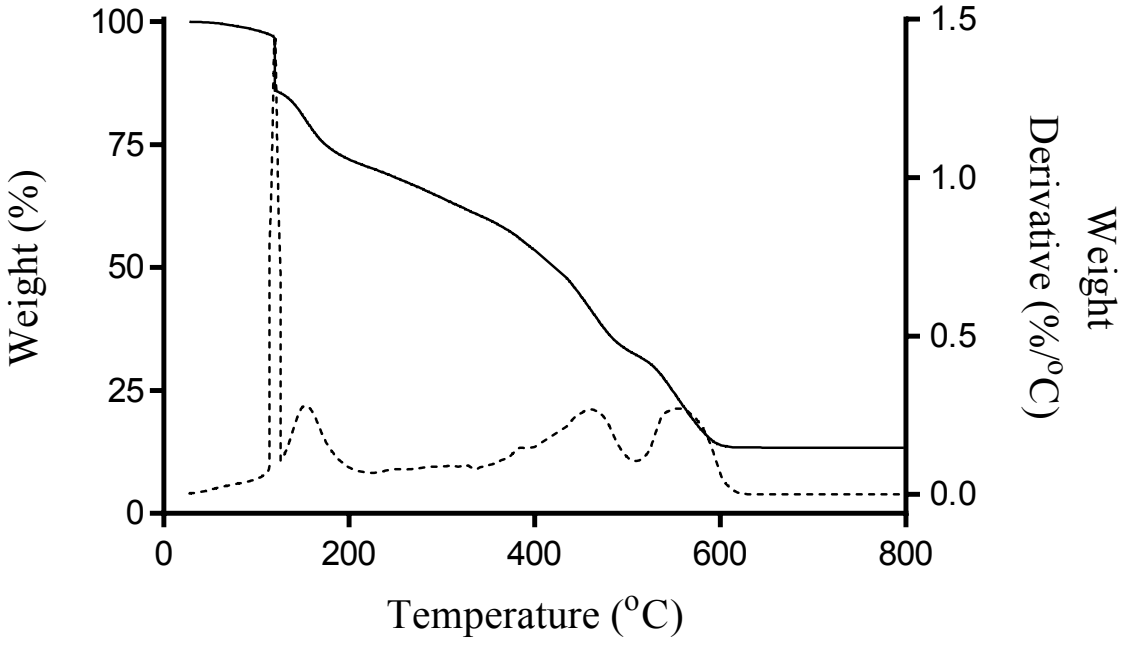

Figure S43: Poly((3aR,7aS)-2-butyl-3a,4,7,7a-tetrahydro-1H-4,7-epoxyisoindole-1,3(2H)-dione$_{80}$-*co*-norbornenylethylisobutyl POSS$^{(R)}{}_{20}$) Poly(**M1**$_{80}$-*co*-**POSS1**$_{20}$) with 10 wt% TiO_2 & AcAc

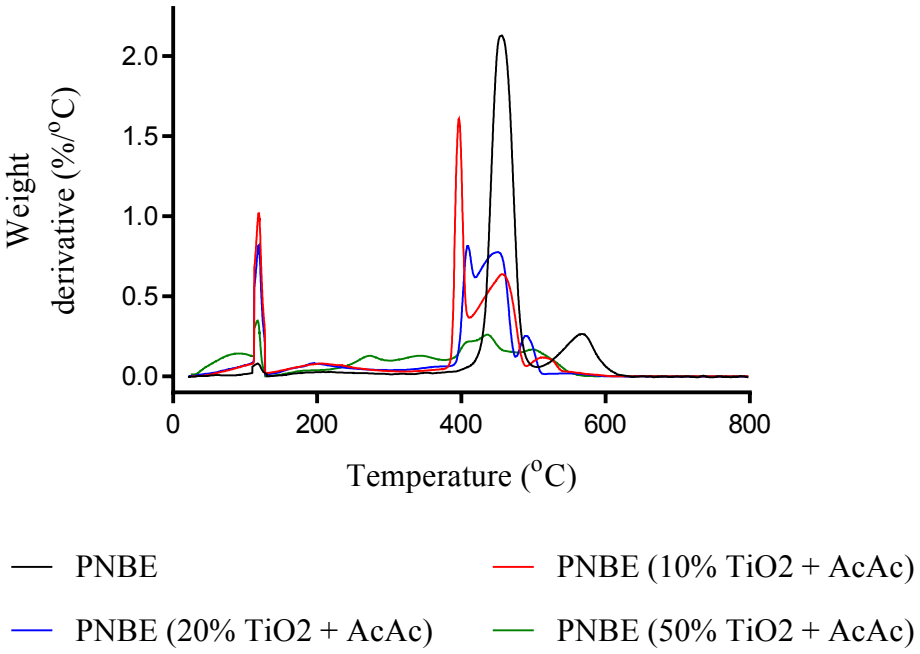

Figure S44: Comparison of weight derivatives for **PNBE** hybrids. The early onset of decomposition for the 10 wt% TiO_2 sample is attributed to titania nanoparticles catalysing thermal degradation. The diminishing effect with increased TiO_2 loading is consistent with the increased domain sizes observed via electron microscopy.

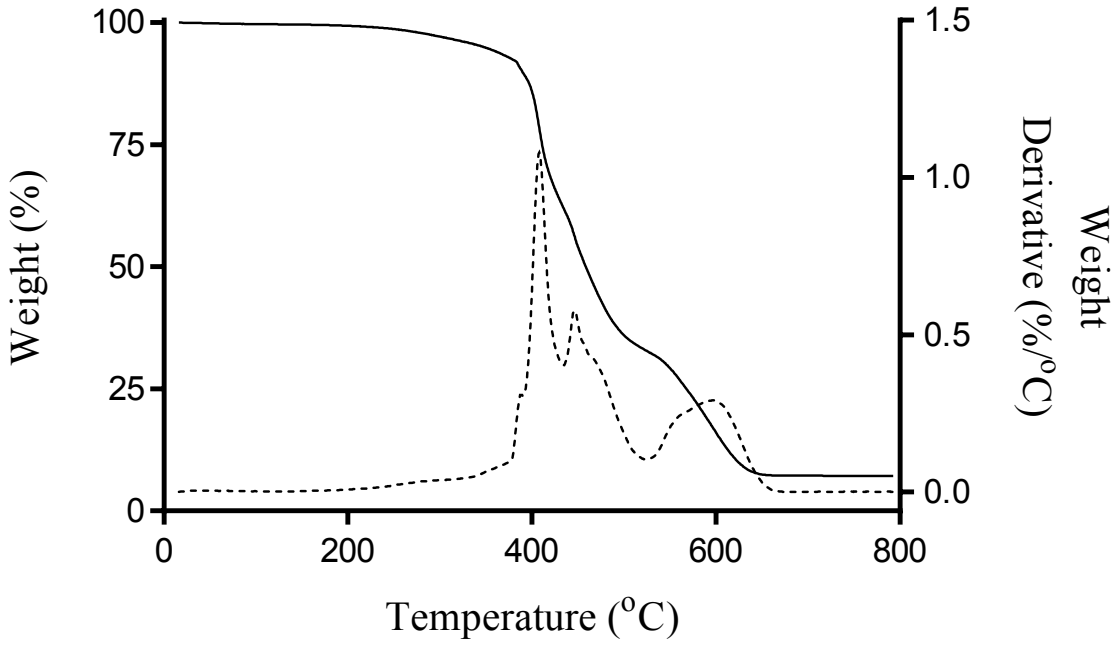

Figure S45: Poly(2-((3a*R*,7a*S*)-1,3-dioxo-3a,4,7,7a-tetrahydro-1*H*-4,7-epoxyisoindol-2(3*H*)-yl)ethyl 3-((3-(triethoxysilyl)propyl)thio)propanoate) poly(**TES**)

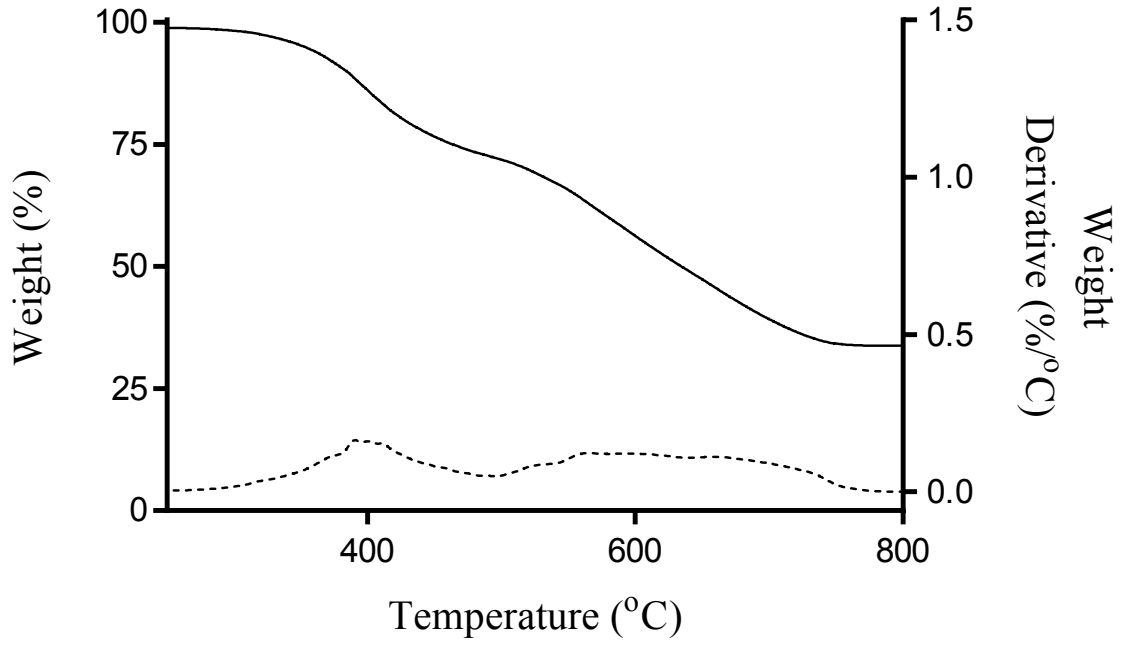

Figure S46: Poly(2-((3a*R*,7a*S*)-1,3-dioxo-3a,4,7,7a-tetrahydro-1*H*-4,7-epoxyisoindol-2(3*H*)-yl)ethyl 3-((3-(triethoxysilyl)propyl)thio)propanoate) poly(**TES**) with 30 wt% TiO_2 & AcAc

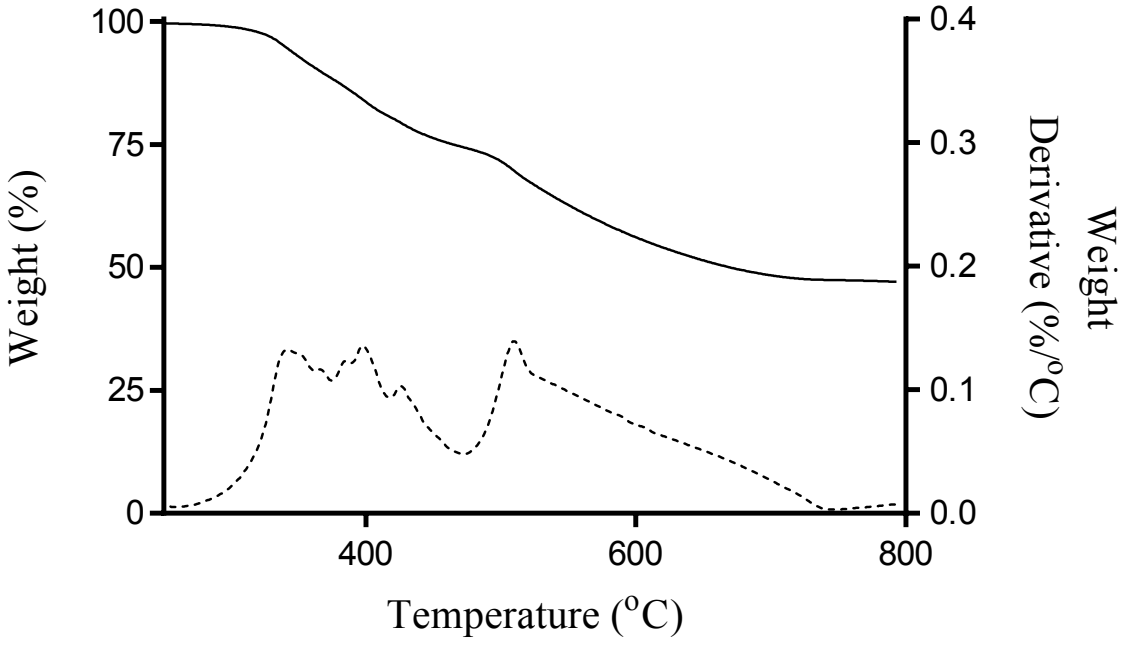

Figure S47: Poly(2-((3a*R*,7a*S*)-1,3-dioxo-3a,4,7,7a-tetrahydro-1*H*-4,7-epoxyisoindol-2(3*H*)-yl)ethyl 3-((3-(triethoxysilyl)propyl)thio)propanoate) poly(**TES**) with 50 wt% TiO_2 & AcAc

4. Additional DMA traces

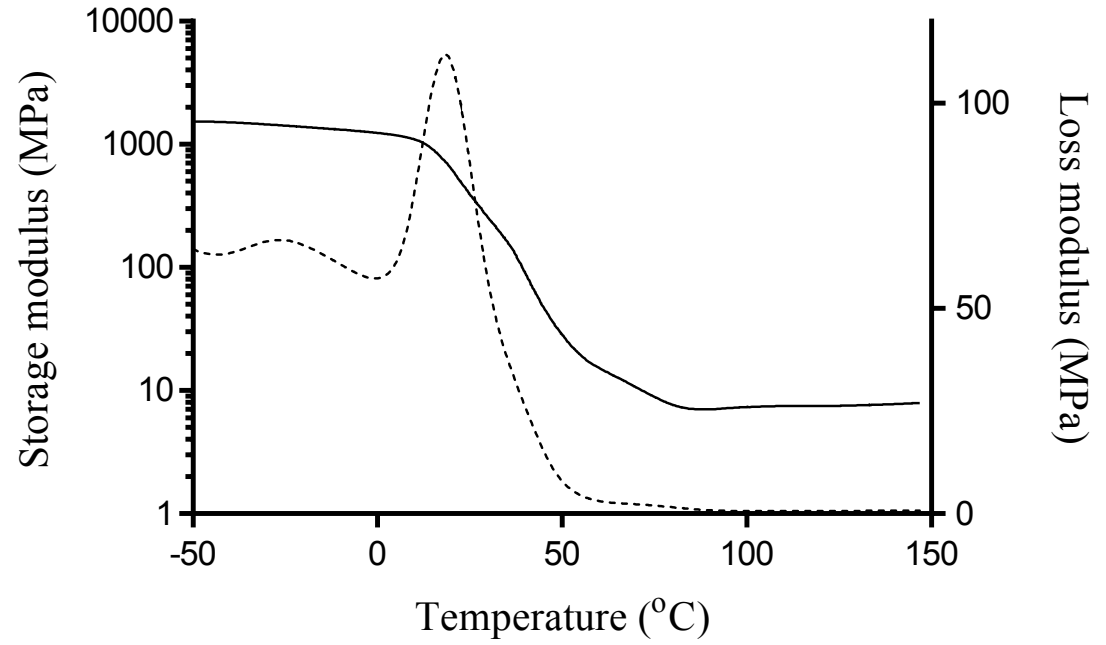

Figure S48: Polynorbornene (**PNBE**)

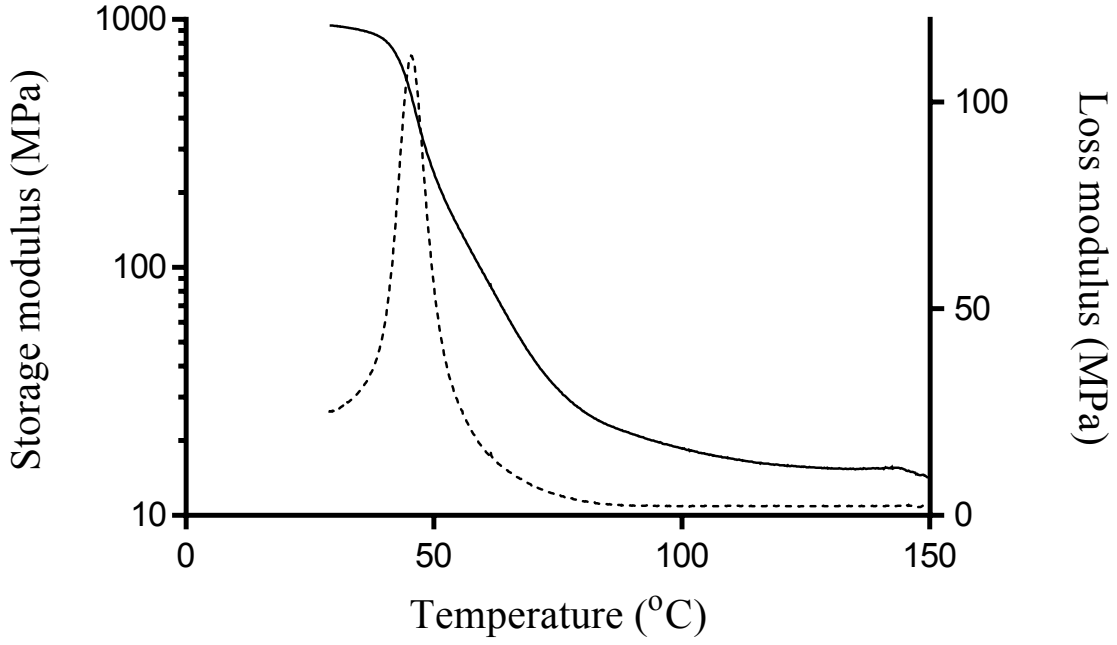

Figure S49: Polynorbornene (**PNBE**) with 10 wt% TiO_2

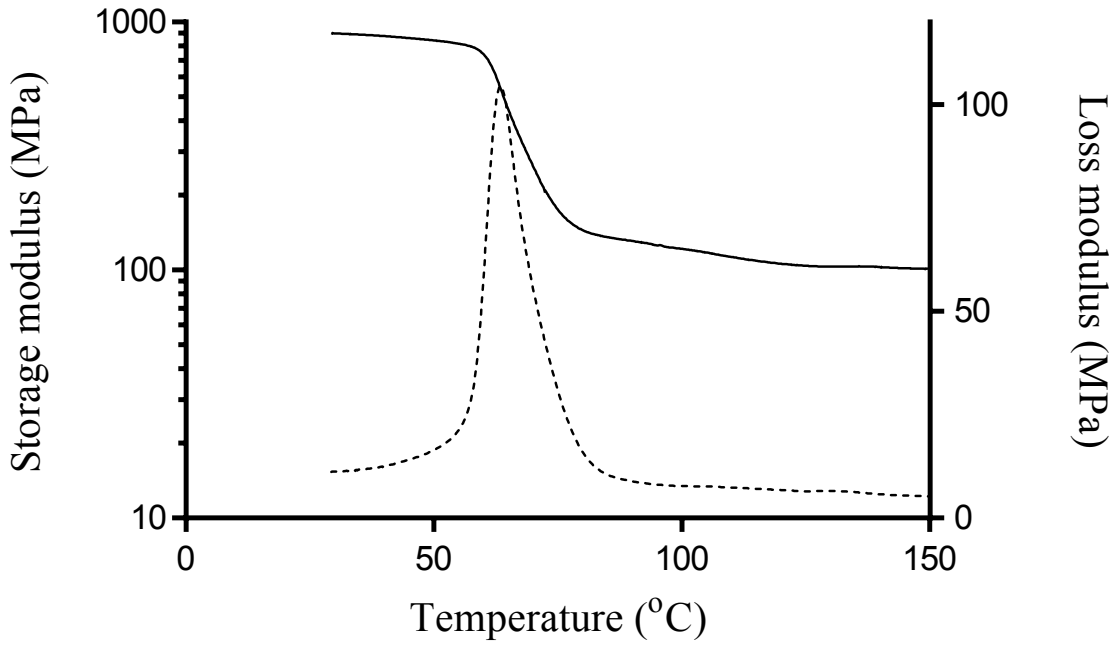

Figure S50: Polynorbornene (**PNBE**) with 20 wt% TiO_2

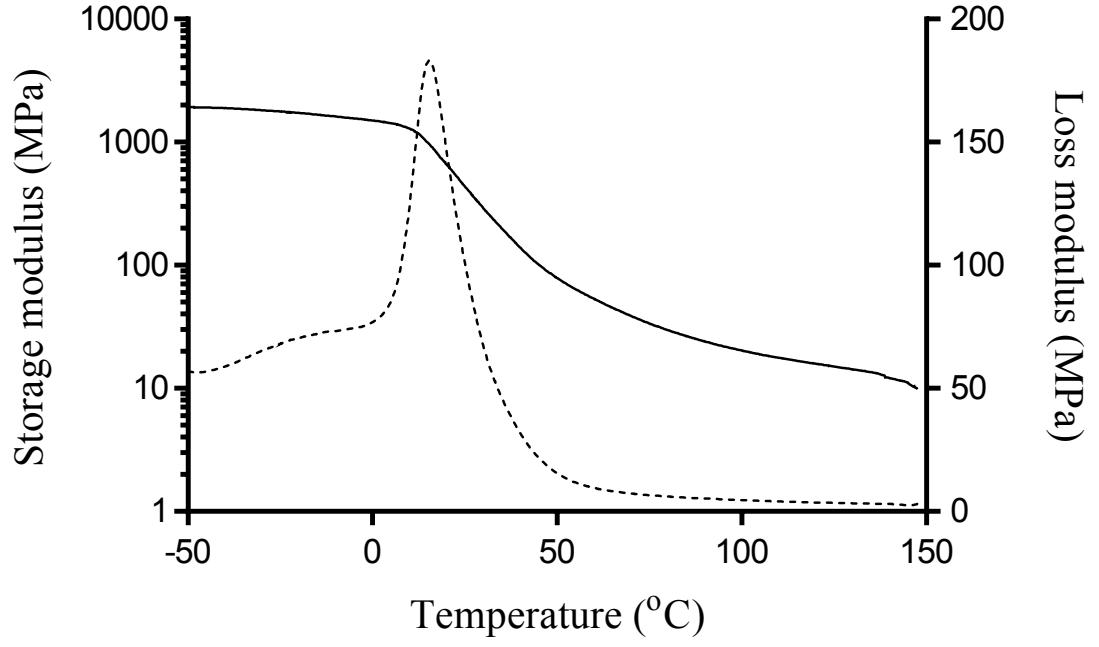

Figure S51: Polynorbornene (**PNBE**) with 10 wt% TiO_2 & AcAc

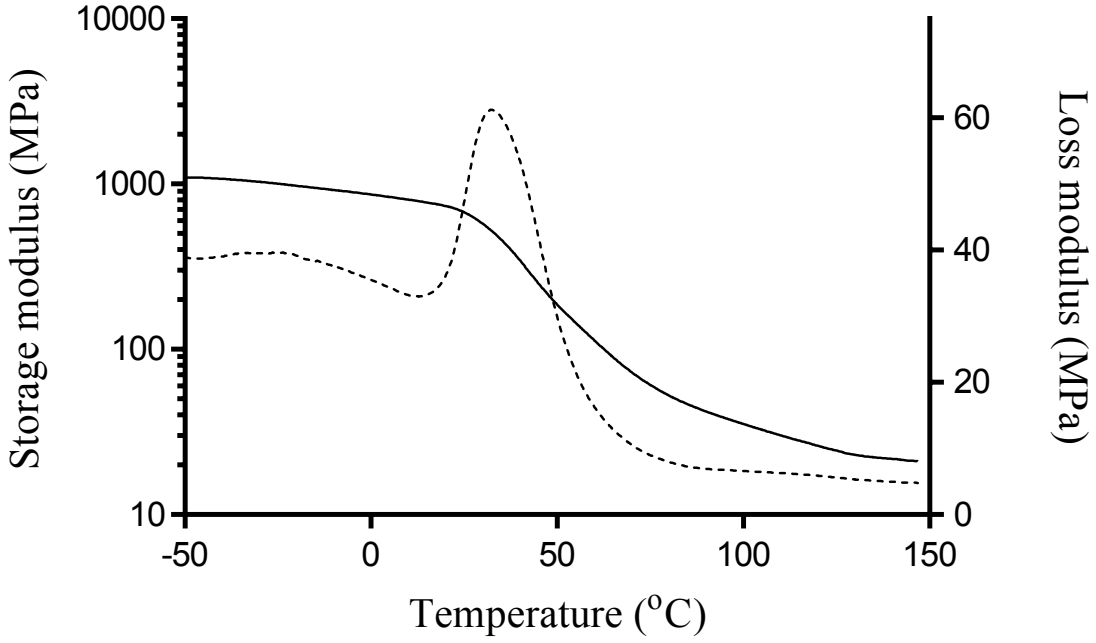

Figure S52: Polynorbornene (**PNBE**) with 20 wt% TiO_2 & AcAc

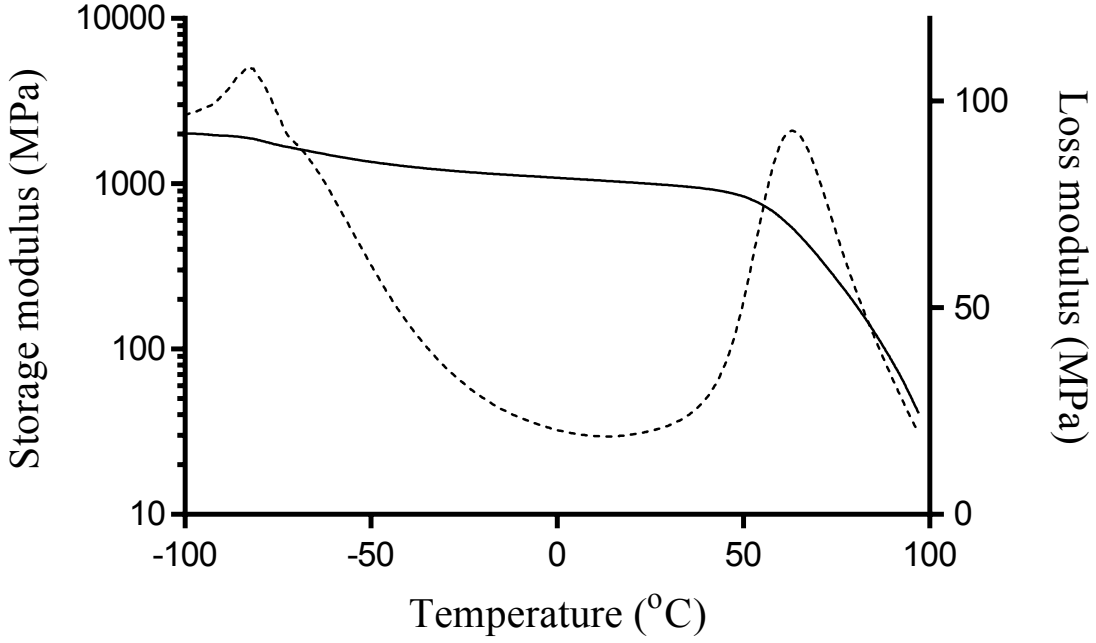

Figure S53: Poly((3aR,7aS)-2-butyl-3a,4,7,7a-tetrahydro-1H-4,7-epoxyisoindole-1,3(2H)-dione) poly(**M1**)

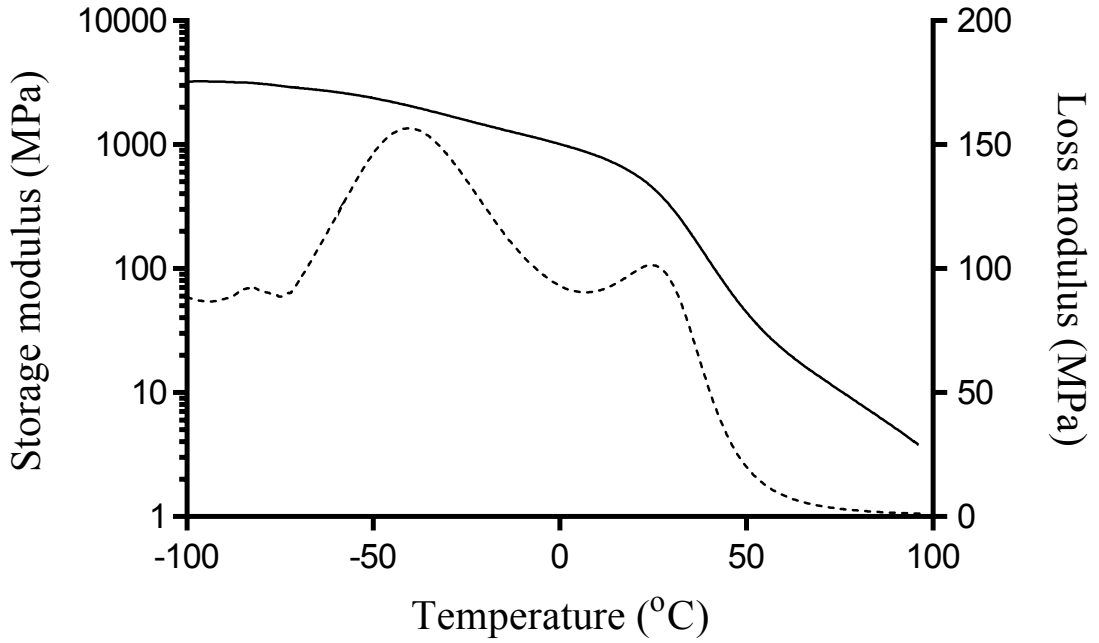

Figure S54: Poly((3aR,7aS)-2-butyl-3a,4,7,7a-tetrahydro-1H-4,7-epoxyisoindole-1,3(2H)-dione) poly(**M1**) with 10 wt% TiO_2 & AcAc

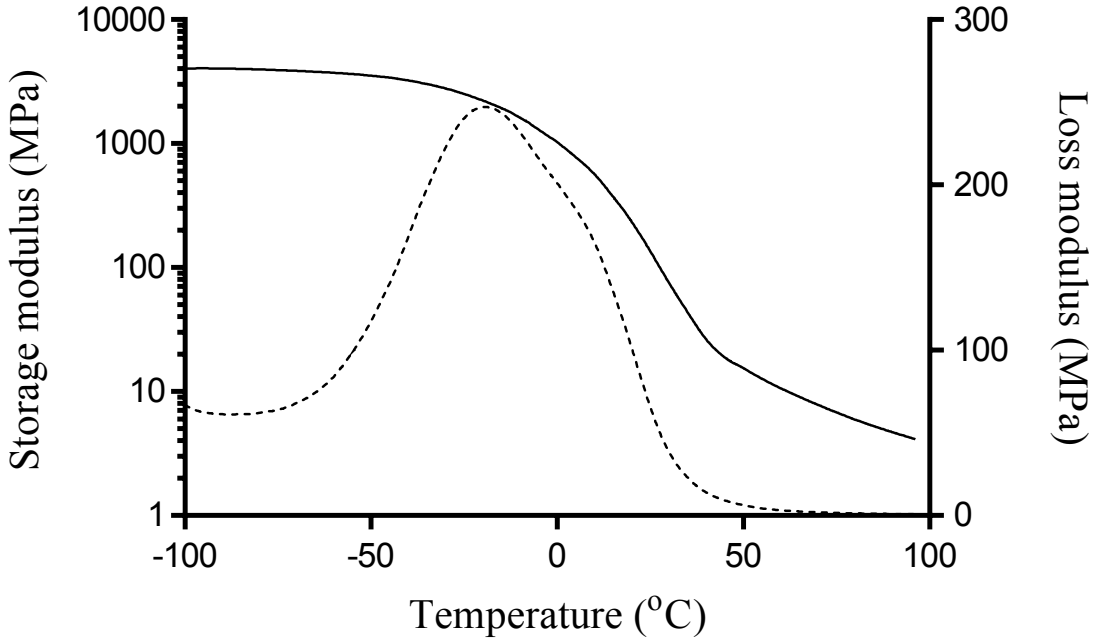

Figure S55: Poly((3aR,7aS)-2-butyl-3a,4,7,7a-tetrahydro-1H-4,7-epoxyisoindole-1,3(2H)-dione$_{80}$-*co*-2-((3aR,7aS)-1,3-dioxo-3a,4,7,7a-tetrahydro-1H-4,7-epoxyisoindol-2(3H)-yl)ethyl 3-((3-(triethoxysilyl)propyl)thio)propanoate$_{20}$) Poly(**M1**$_{80}$-*co*-**TES**$_{20}$) with 10 wt% TiO_2 & AcAc

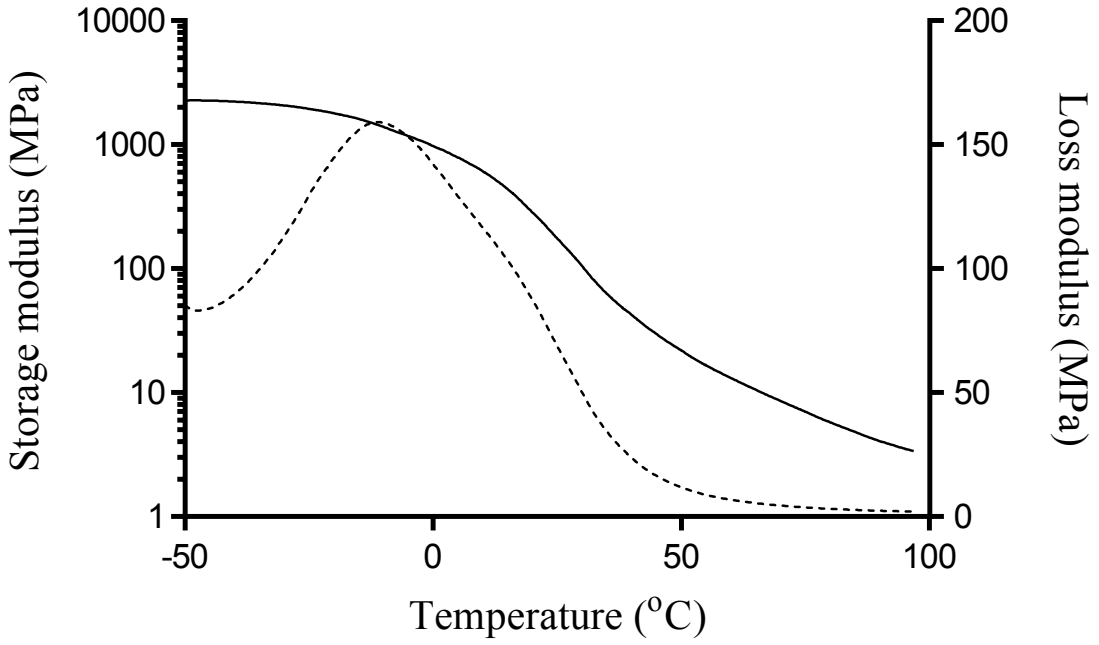

Figure S56: Poly((3aR,7aS)-2-butyl-3a,4,7,7a-tetrahydro-1H-4,7-epoxyisoindole-1,3(2H)-dione$_{80}$-*co*-norbornenylethylisobutyl POSS$^{(R)}{}_{20}$) Poly(**M1**$_{80}$-*co*-**POSS1**$_{20}$) with 10 wt% TiO_2 & AcAc

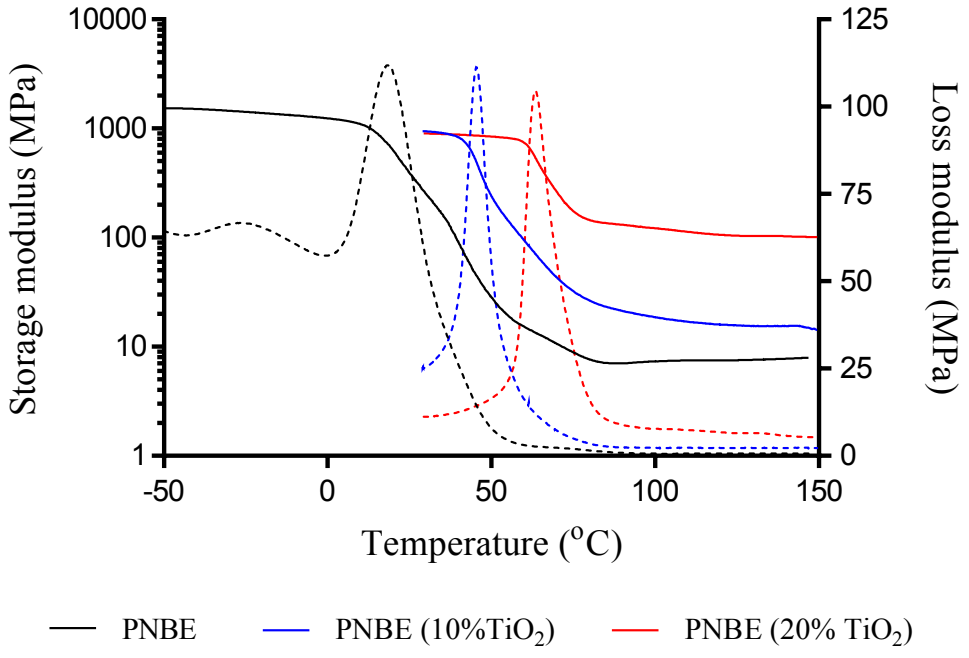

Figure S57: Comparison of **PNBE** with varying loadings of TiO_2.
This figure demonstrates a clear relationship between glass transition and titania loading, consistent with established literature.

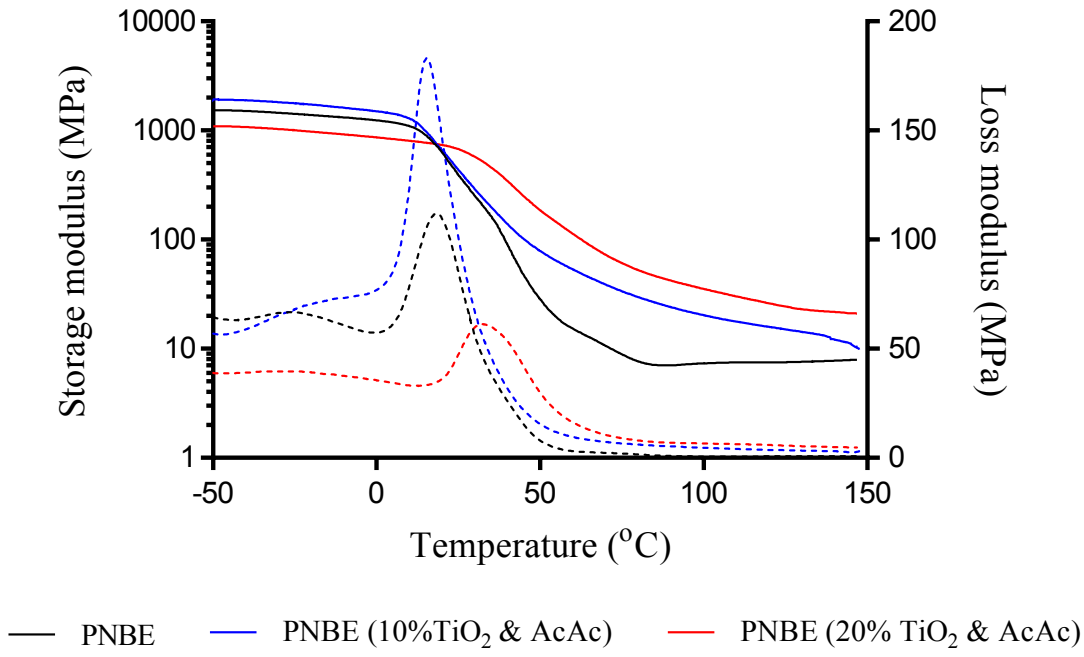

Figure S58: Comparison of **PNBE** prepared with AcAc and with varying loadings of TiO_2. The unusual behaviour exhibited by the 10% TiO_2 sample (negligible increase in T_g and elevated modulus) is attributed to the nano-scale domains versus the micrometer-scale domains of the samples with higher loadings and the samples prepared without AcAc.

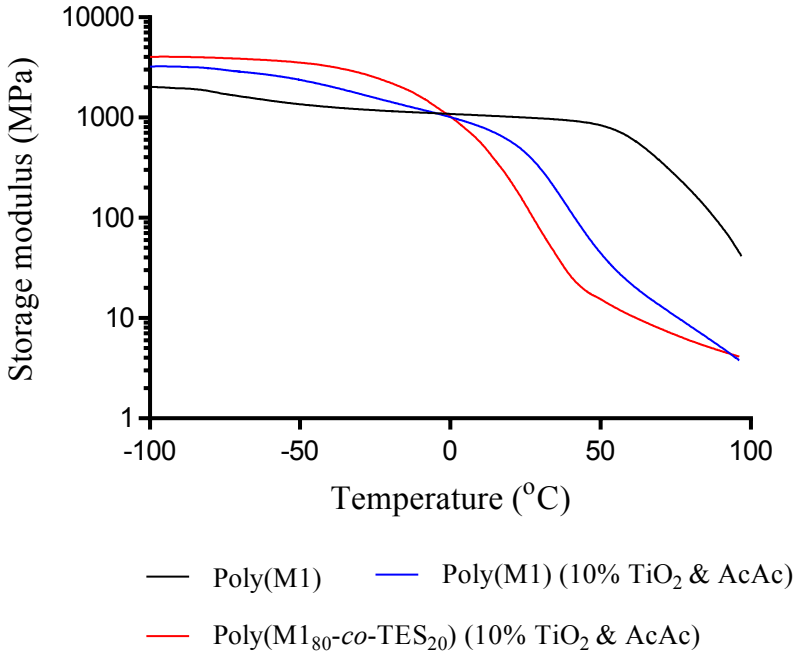

Figure S59: Comparison of poly(**M1**) hybrids. The addition of nano-scale TiO_2 increases modulus over the unfilled polymer. The modulus further increases with the introduction of covalent bonds *via* the TES comonomer.

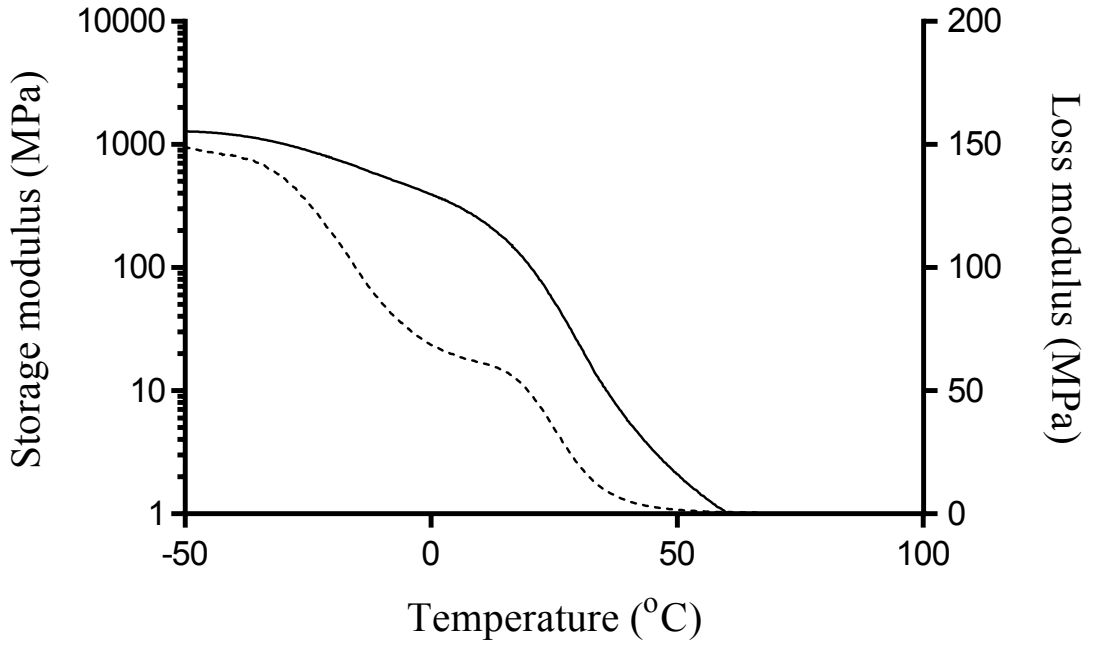

Figure S60: Poly(2-((3a*R*,7a*S*)-1,3-dioxo-3a,4,7,7a-tetrahydro-1*H*-4,7-epoxyisoindol-2(3*H*)-yl)ethyl 3-((3-(triethoxysilyl)propyl)thio)propanoate) poly(**TES**)

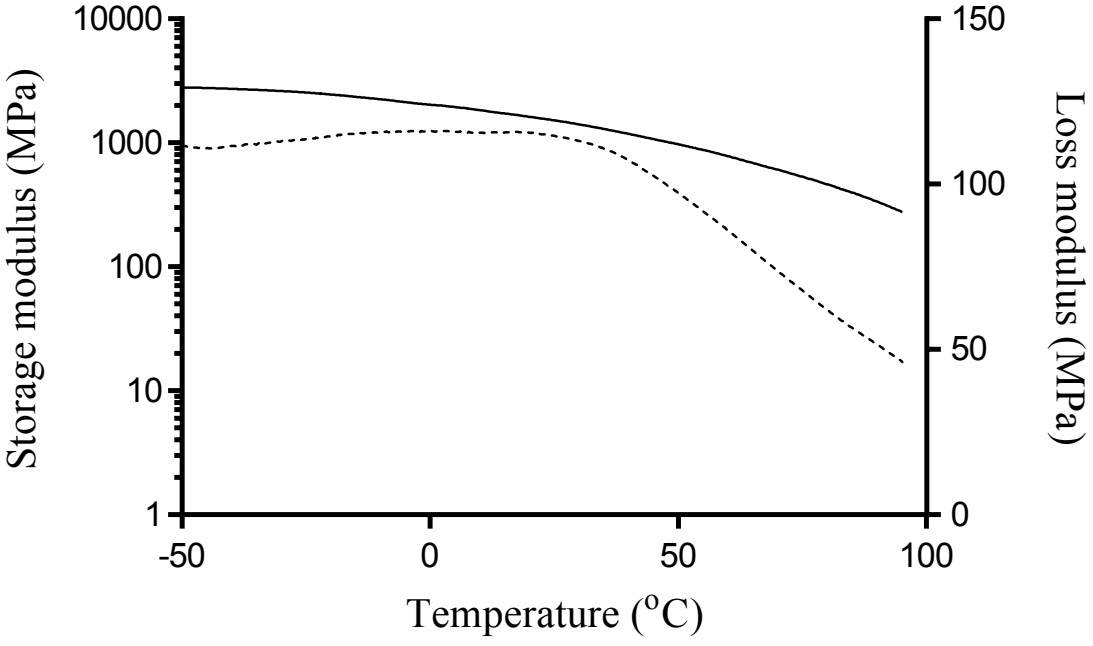

Figure S61: Poly(2-((3a*R*,7a*S*)-1,3-dioxo-3a,4,7,7a-tetrahydro-1*H*-4,7-epoxyisoindol-2(3*H*)-yl)ethyl 3-((3-(triethoxysilyl)propyl)thio)propanoate) poly(**TES**) with 10 wt% TiO_2.

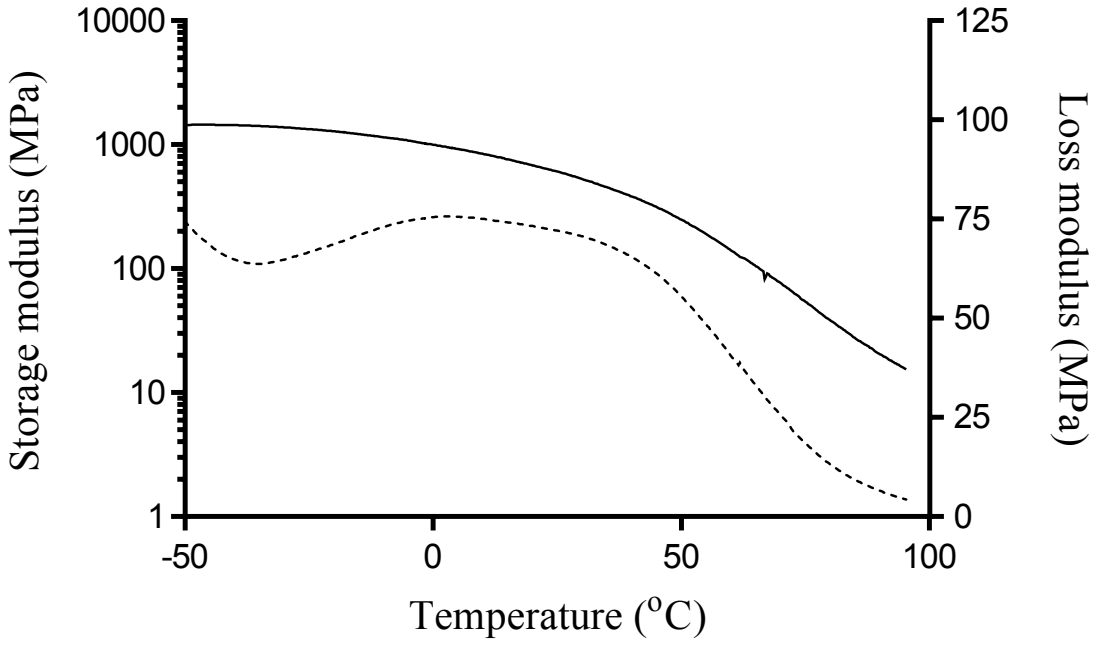

Figure S62: Poly(2-((3a*R*,7a*S*)-1,3-dioxo-3a,4,7,7a-tetrahydro-1*H*-4,7-epoxyisoindol-2(3*H*)-yl)ethyl 3-((3-(triethoxysilyl)propyl)thio)propanoate) poly(**TES**) with 20 wt% TiO_2.

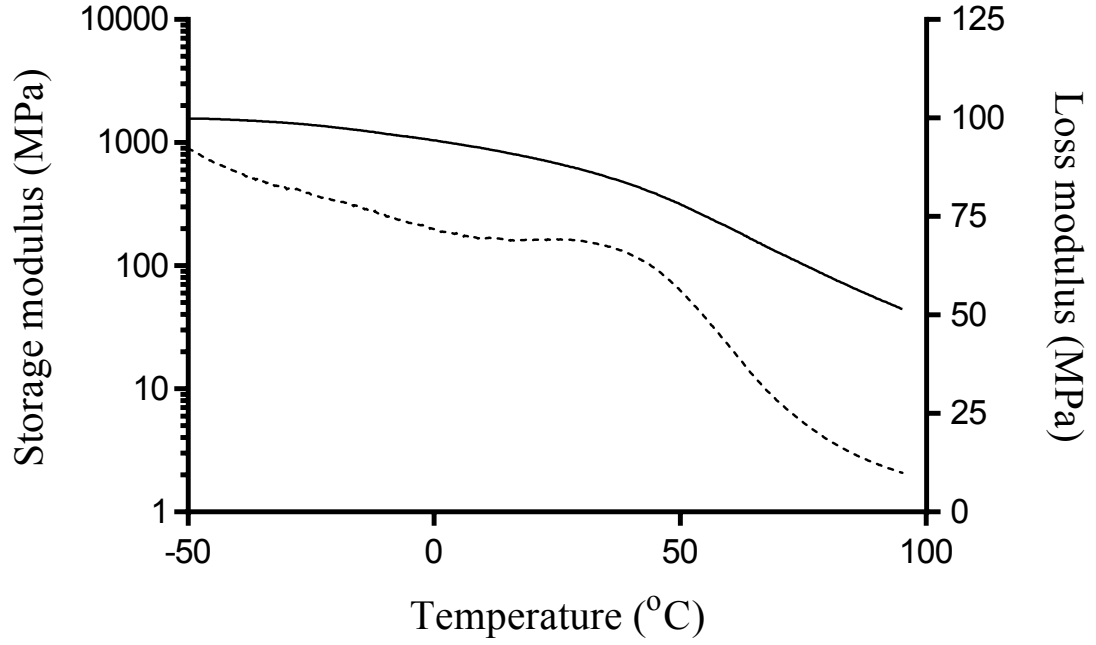

Figure S63: Poly(2-((3a*R*,7a*S*)-1,3-dioxo-3a,4,7,7a-tetrahydro-1*H*-4,7-epoxyisoindol-2(3*H*)-yl)ethyl 3-((3-(triethoxysilyl)propyl)thio)propanoate) poly(**TES**) with 30 wt% TiO_2.

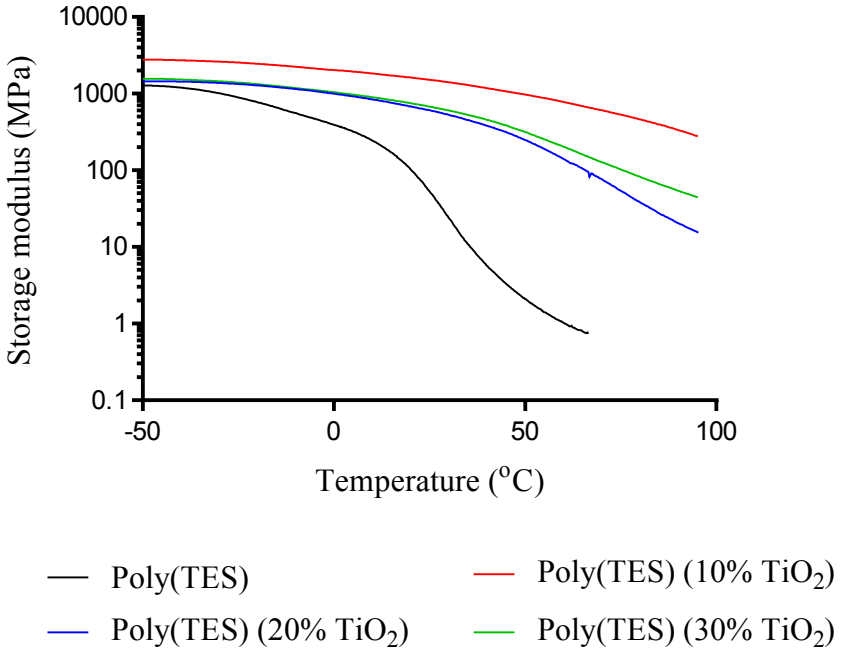

Figure S64: Comparison of poly(**TES**) hybrids. The addition of nano-scale TiO_2 increases modulus over the unfilled polymer. The unusually high modulus of the 10% TiO_2 sample is attributed to a higher density and higher effective sample thickness versus the 20 and 30% samples which exhibit some porosity due to residual solvent. The effect is accentuated as the sample dimensions are raised to the third order in the modulus calculations.

5. FTIR spectra of polymers and hybrids

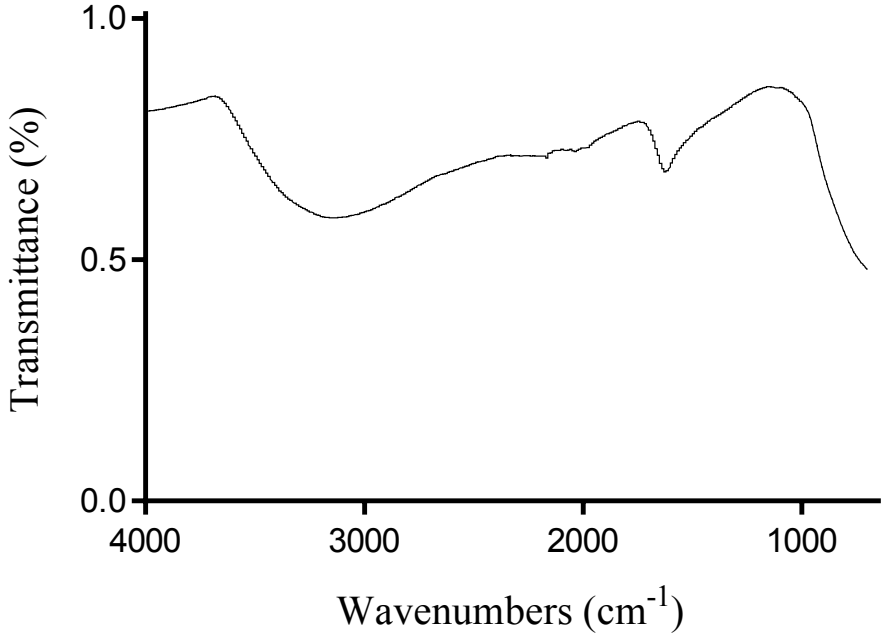

Figure S65: Titania (**TiO_2**)

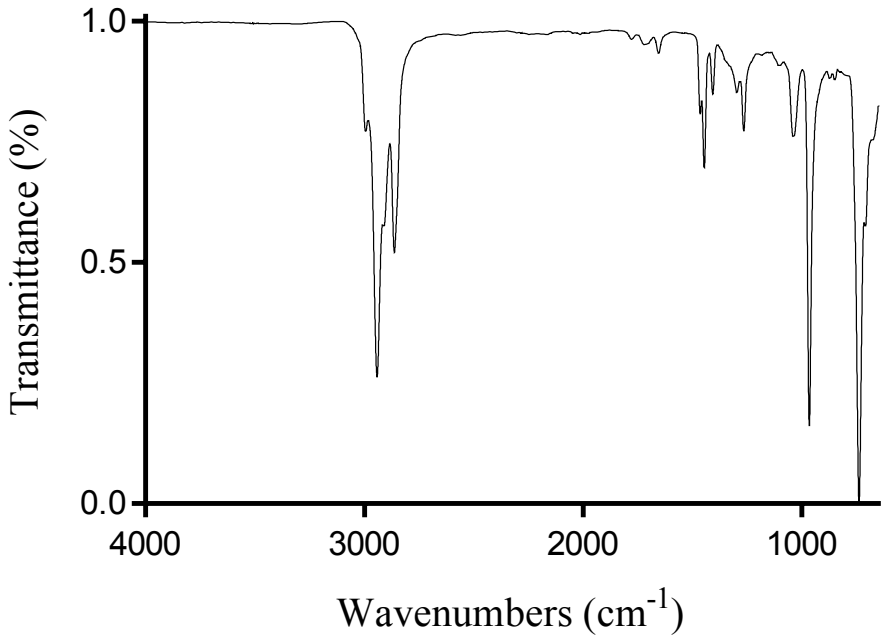

Figure S66: Polynorbornene (**PNBE**)

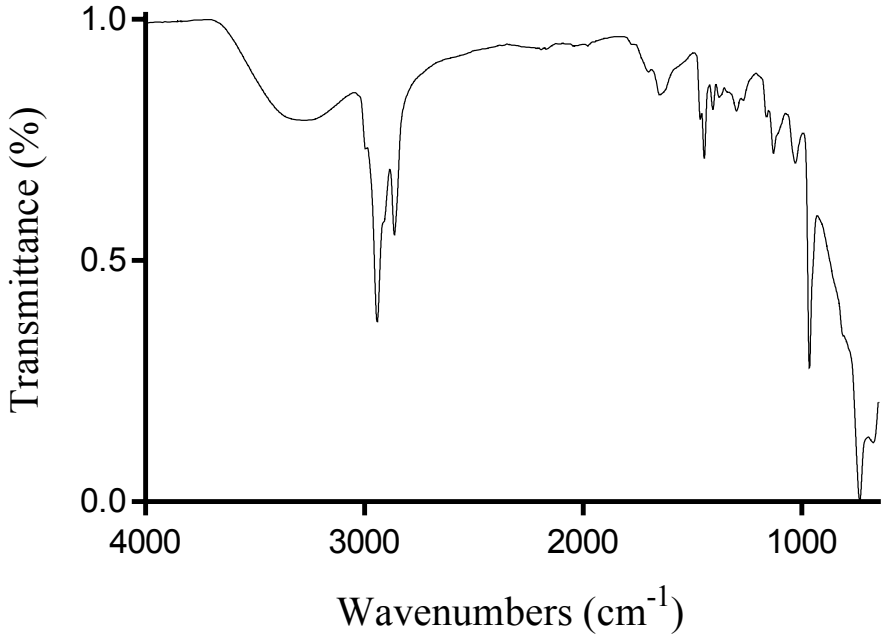

Figure S67: Polynorbornene (**PNBE**) with 10 wt% TiO_2

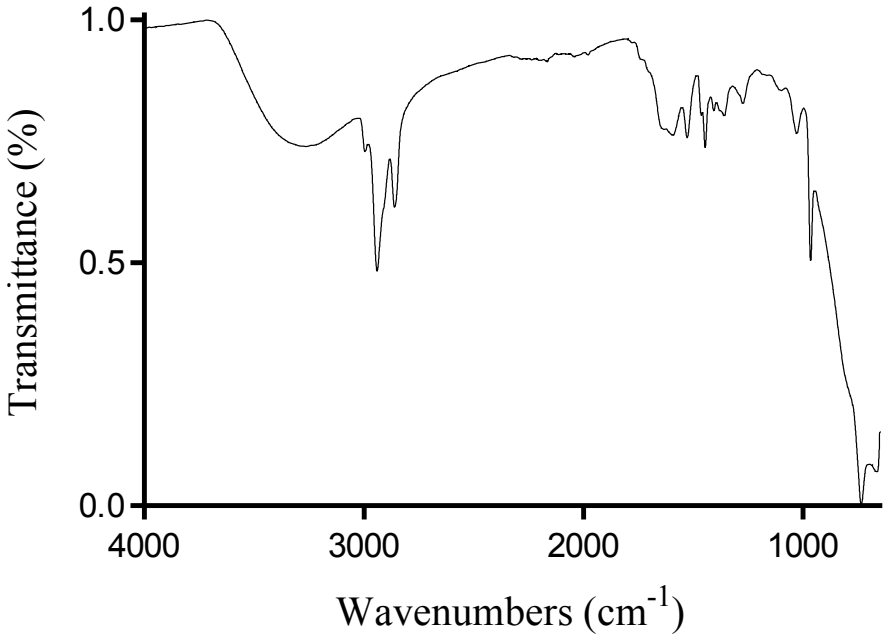

Figure S68: Polynorbornene (**PNBE**) with 20 wt% TiO_2

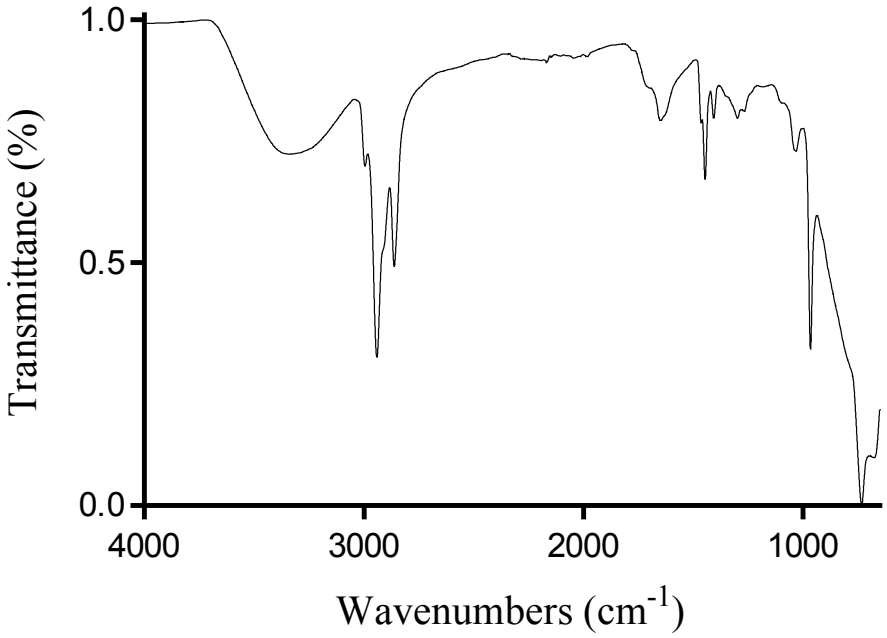

Figure S69: Polynorbornene (**PNBE**) with 50 wt% TiO_2

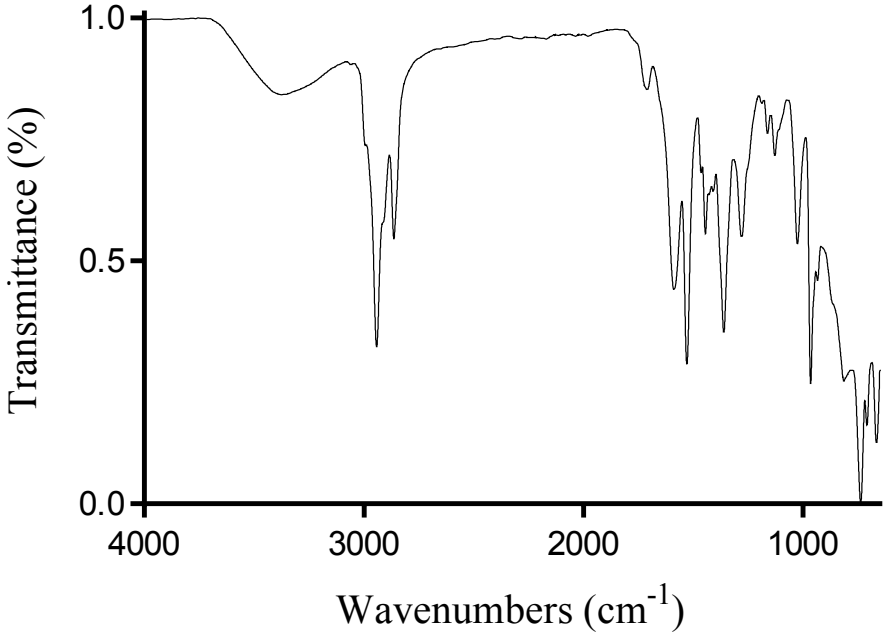

Figure S70: Polynorbornene (**PNBE**) with 10 wt% TiO_2 & AcAc

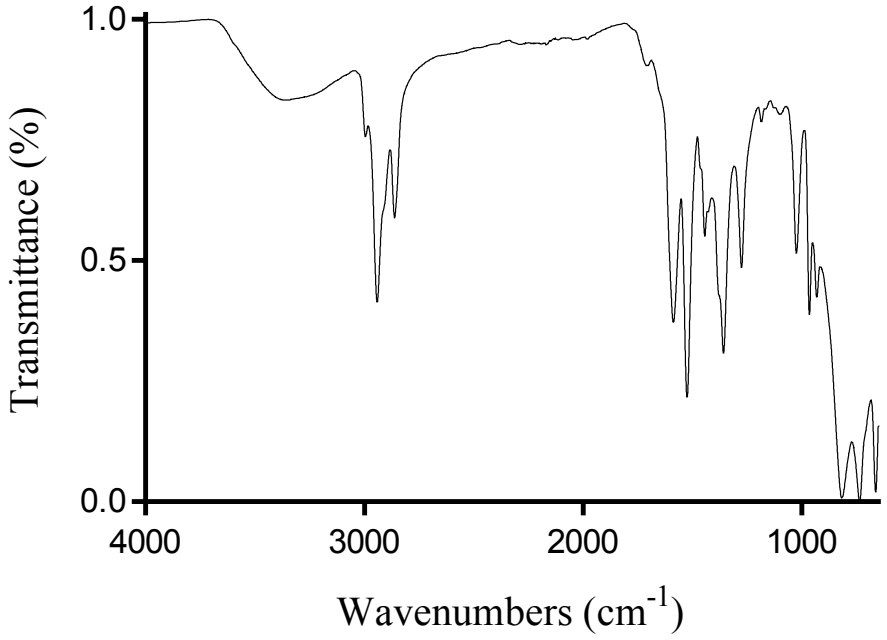

Figure S71: Polynorbornene (**PNBE**) with 20 wt% TiO_2 & AcAc

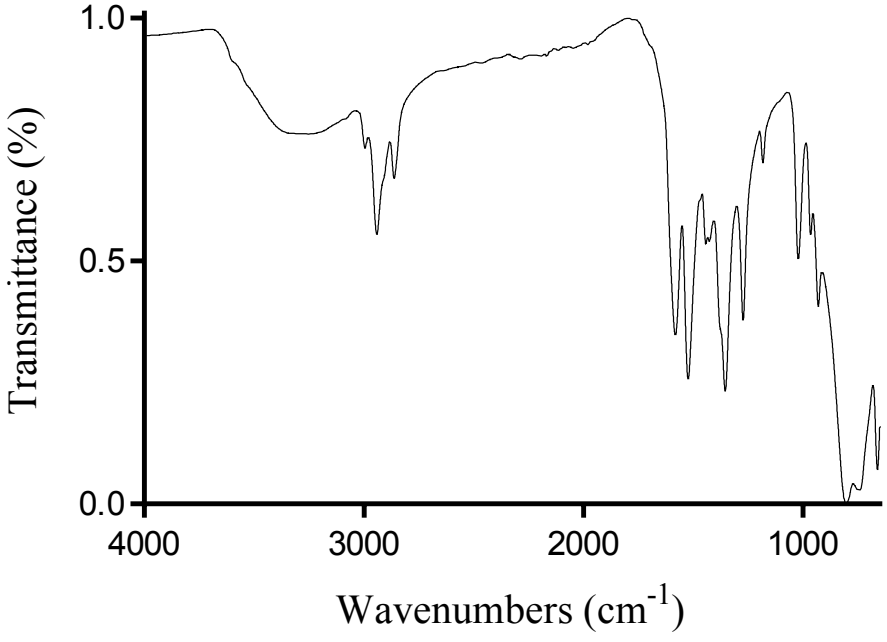

Figure S72: Polynorbornene (**PNBE**) with 50 wt% TiO_2 & AcAc

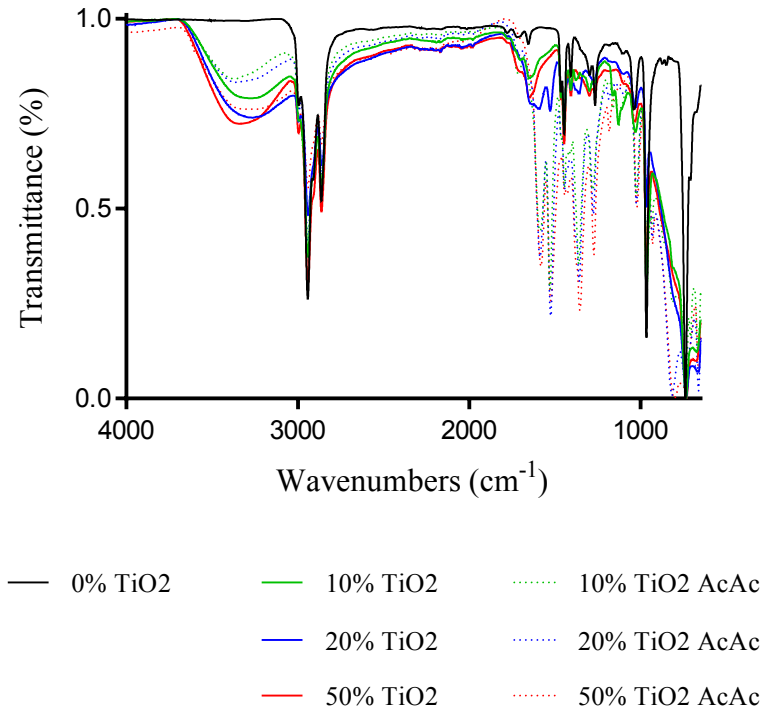

Figure S73: Comparison of **PNBE** and its hybrids

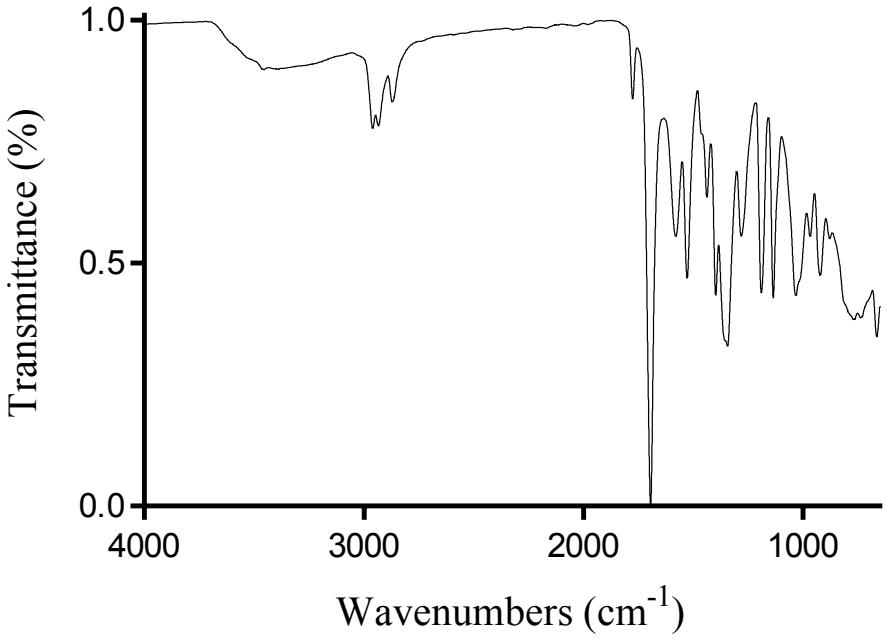

Figure S74: Poly((3aR,7aS)-2-butyl-3a,4,7,7a-tetrahydro-1H-4,7-epoxyisoindole-1,3(2H)-dione) poly(**M1**) with 10 wt% TiO_2 & AcAc

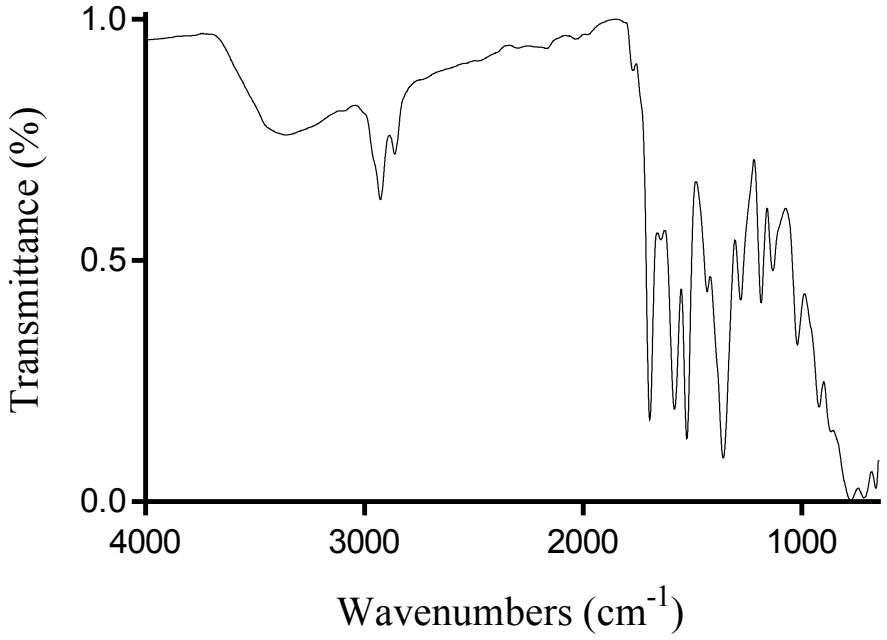

Figure S75: Poly((3aR,7aS)-2-butyl-3a,4,7,7a-tetrahydro-1H-4,7-epoxyisoindole-1,3(2H)-dione$_{80}$-*co*-2-((3aR,7aS)-1,3-dioxo-3a,4,7,7a-tetrahydro-1H-4,7-epoxyisoindol-2(3H)-yl)ethyl 3-((3-(triethoxysilyl)propyl)thio)propanoate$_{20}$) Poly(**M1**$_{80}$-*co*-**TES**$_{20}$) with 10 wt% TiO_2 & AcAc

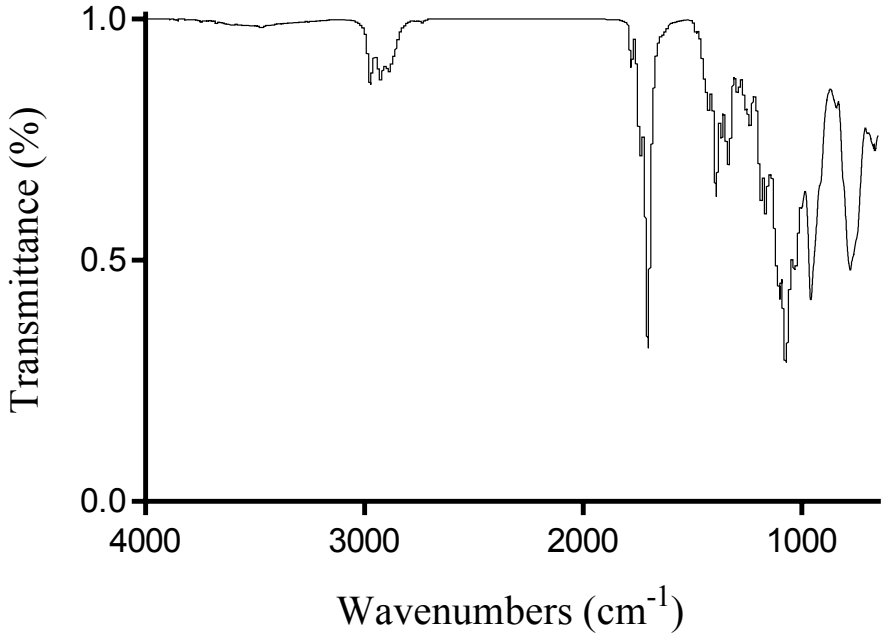

Figure S76: Poly(2-((3a*R*,7a*S*)-1,3-dioxo-3a,4,7,7a-tetrahydro-1*H*-4,7-epoxyisoindol-2(3*H*)-yl)ethyl 3-((3-(triethoxysilyl)propyl)thio)propanoate) poly(**TES**)

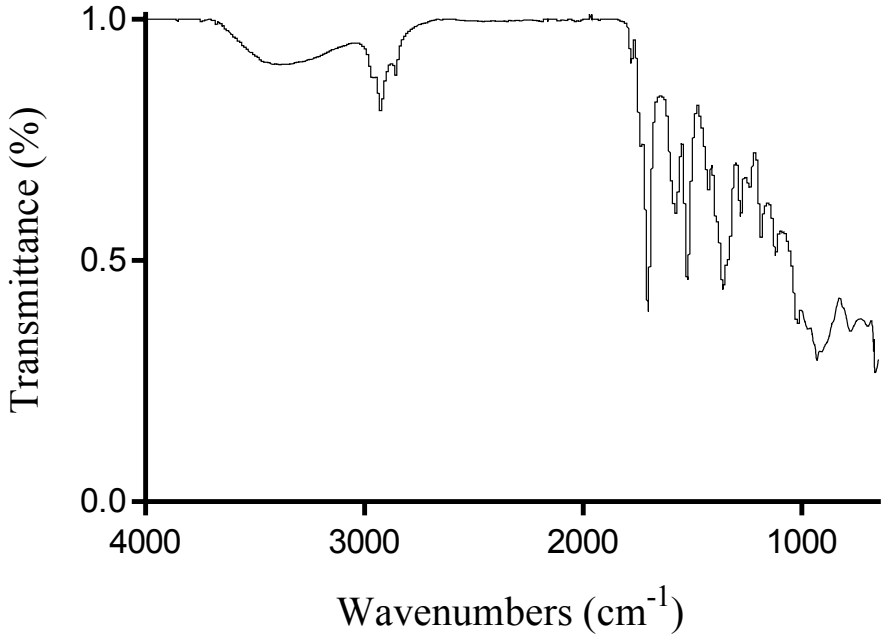

Figure S77: Poly(2-((3a*R*,7a*S*)-1,3-dioxo-3a,4,7,7a-tetrahydro-1*H*-4,7-epoxyisoindol-2(3*H*)-yl)ethyl 3-((3-(triethoxysilyl)propyl)thio)propanoate) poly(**TES**) with 10 wt% TiO_2 & AcAc

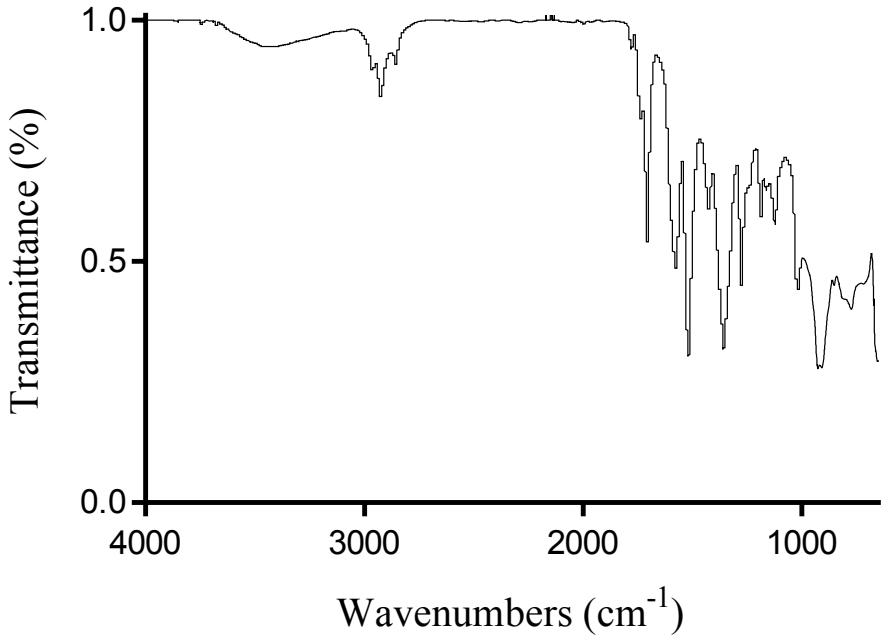

Figure S78: Poly(2-((3a*R*,7a*S*)-1,3-dioxo-3a,4,7,7a-tetrahydro-1*H*-4,7-epoxyisoindol-2(3*H*)-yl)ethyl 3-((3-(triethoxysilyl)propyl)thio)propanoate) poly(**TES**) with 20 wt% TiO_2 & AcAc

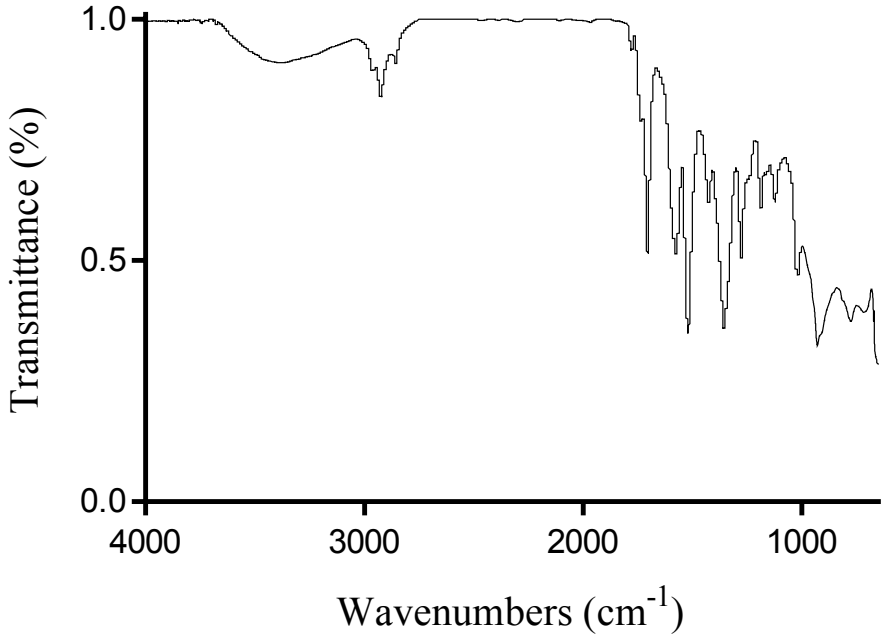

Figure S79: Poly(2-((3a*R*,7a*S*)-1,3-dioxo-3a,4,7,7a-tetrahydro-1*H*-4,7-epoxyisoindol-2(3*H*)-yl)ethyl 3-((3-(triethoxysilyl)propyl)thio)propanoate) poly(**TES**) with 30 wt% TiO_2 & AcAc

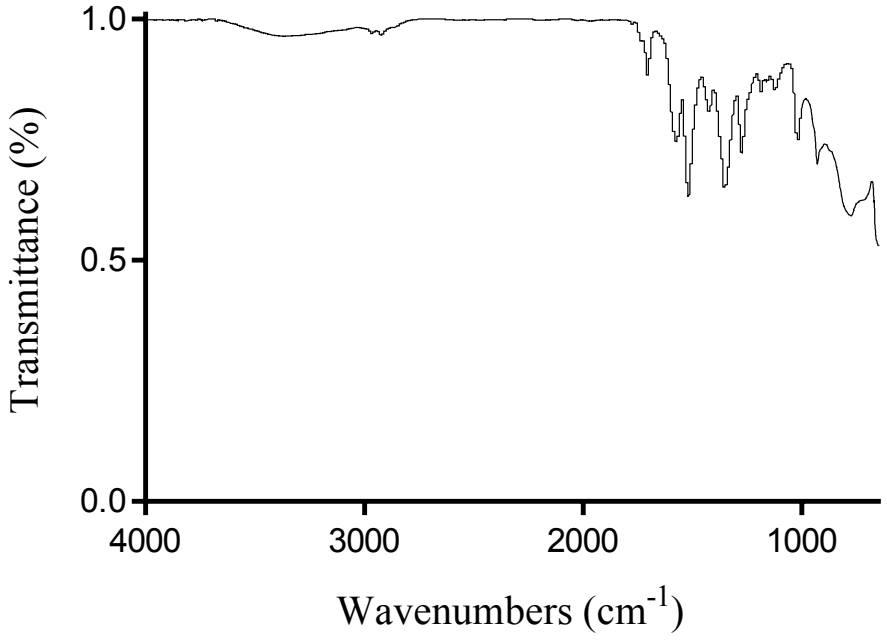

Figure S80: Poly(2-((3a*R*,7a*S*)-1,3-dioxo-3a,4,7,7a-tetrahydro-1*H*-4,7-epoxyisoindol-2(3*H*)-yl)ethyl 3-((3-(triethoxysilyl)propyl)thio)propanoate) poly(**TES**) with 50 wt% TiO_2 & AcAc

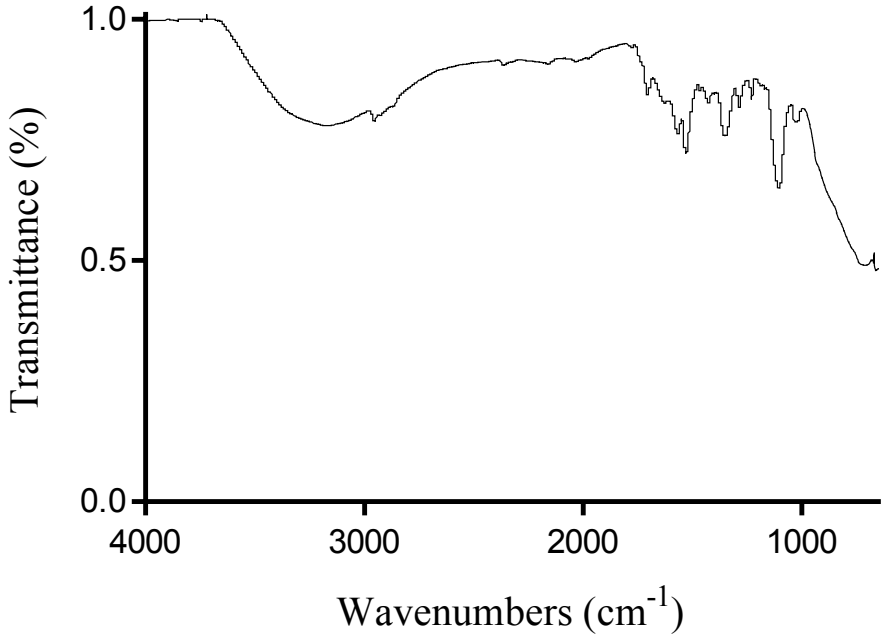

Figure S81: Poly(norbornenylethylisobutyl POSS$^{(R)}_{50}$-*co*-2-((3a*R*,7a*S*)-1,3-dioxo-3a,4,7,7a-tetrahydro-1*H*-4,7-epoxyisoindol-2(3*H*)-yl)ethyl 3-((3-(triethoxysilyl)propyl) thio)propanoate$_{50}$) poly(**POSS1**$_{50}$-*co*-**TES**$_{50}$) with 50 wt% TiO_2 & AcAc

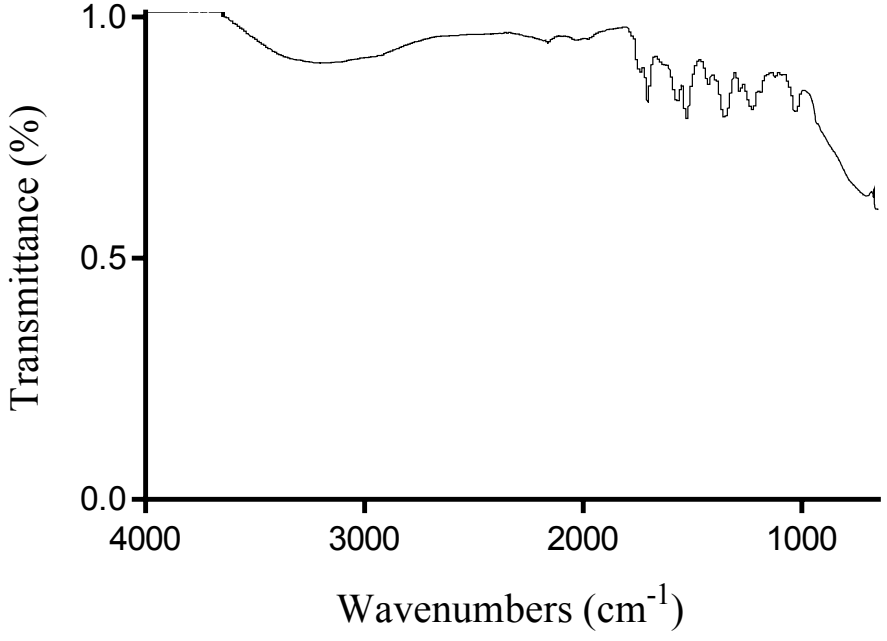

Figure S82: Poly((2S,3S,4S,5R,6R)-6-((3-(2-((3aR,7aS)-1,3-dioxo-1,3,3a,4,7,7a-hexahydro-2H-4,7-epoxyisoindol-2-yl)ethoxy)-3-oxopropyl)thio)tetrahydro-2H-pyran-2,3,4,5-tetrayltetraacetate$_{50}$-*co*-2-((3a*R*,7a*S*)-1,3-dioxo-3a,4,7,7a-tetrahydro-1*H*-4,7-epoxyisoindol-2(3*H*)-yl)ethyl 3-((3-(triethoxysilyl)propyl) thio)propanoate$_{50}$) poly(**M5**$_{50}$-*co*-**TES**$_{50}$) with 50 wt% TiO_2 & AcAc

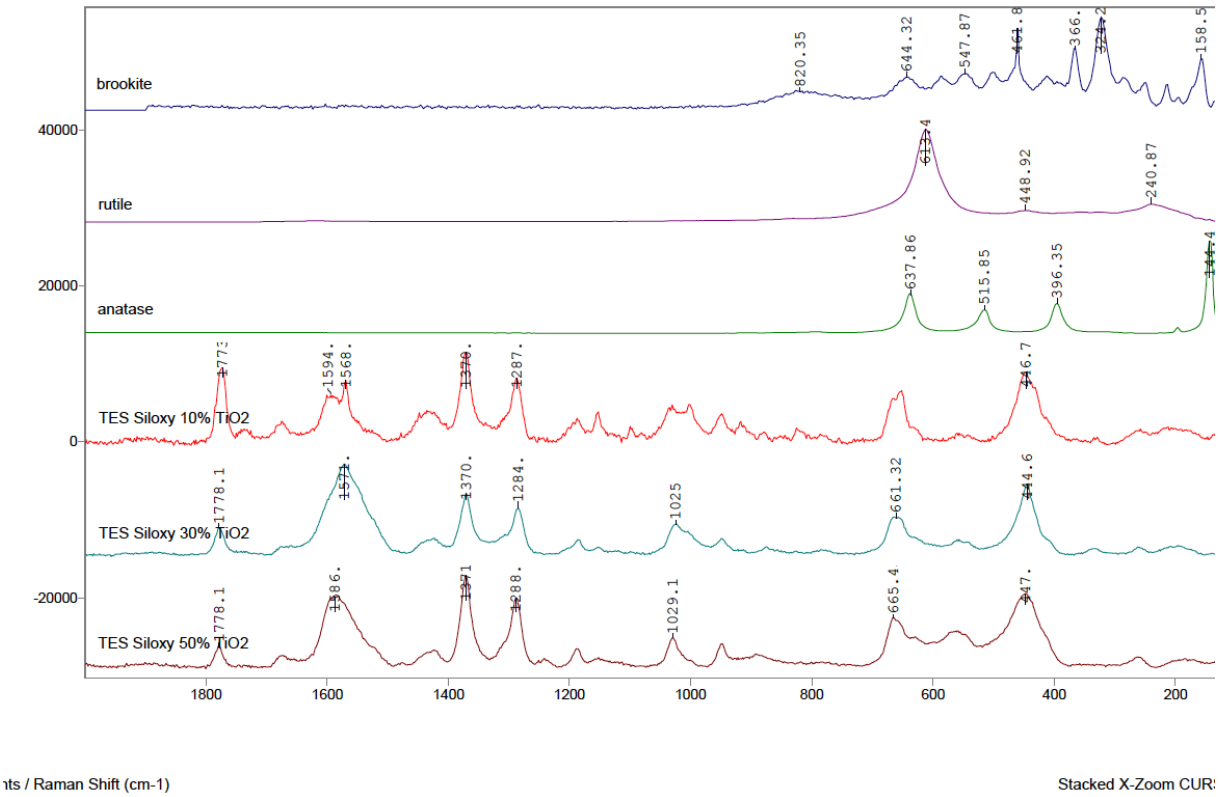

Figure S83. Raman spectra of three basic crystalline forms of titania and examples of **TES**-Ti hybrids